

ABSTRACT

HENRY, ERIC. Regenerative Potential of Adult Lung Spheroid Cells in a Bleomycin-Induced Pulmonary Fibrosis Rodent Model. (Under the direction of Ke Cheng).

Chronic lung diseases, such as pulmonary fibrosis, are devastating conditions which drastically effect the overall quality of life of the patients who suffer from them. Many of these diseases are progressive and over time degenerate the lung to the point where the patient requires drastic and invasive measures such as a lung transplant. Currently there is no cure for progressive lung diseases. New methods are being researched to provide patients with more therapeutic options. Stem cell therapies have shown promise in the treatment of many conditions, including lung diseases, with many clinical trials currently under investigation in the United States. Most, if not all, trials use mesenchymal stem cells (MSCs) from other parts of the body (e.g. adipose, bone marrow) which require specific stimuli to control the stem cells down desired differentiation pathways. Using endogenous lung stem cells instead of MSCs minimizes the stimulus required for differentiation as these cells are from the lungs and predestined for differentiation into mature lung cells. In this thesis study, adult lung stem cells were derived from healthy lung tissue explants using a simple three dimensional spheroid culture system. The spheroid culture process has been widely applied in culturing neural and cardiac stem cells. The resulting cell products, namely lung spheroid cells or LSCs, were analyzed *in vitro* and *in vivo* for their regenerative potential in pulmonary fibrosis. Phenotyping of the cells was performed using immunofluorescence and flow cytometry. A bleomycin induced pulmonary fibrosis rodent model was generated to test regenerative potential of LSCs. Media conditioned by the LSCs was gathered and analyzed to identify potential protein secretions which may have positive paracrine effects on the lung tissues *in vivo*.

As a result, LSCs were shown to be effectively grown into large numbers using the spheroid culture process. Phenotypically, LSCs express proteins which are known to correlate with adult lung stem cell populations, such as prosurfactant protein C (Pro-SP-C) for alveolar type II (ATII) cells and club cell secretory protein (CCSP) for club cells. Due to the nature of LSCs expansion, other cell types are also present in during the culture process, specifically CD105 and CD90 positive cells, which assist in recapitulating the lung stromal environment in culture. In a rodent model of pulmonary fibrosis, LSC treated lungs showed decreased fibrosis, tissue infiltrates, and increased angiogenesis histologically in comparison to control-treated animals. While benefits are striking, only limited numbers of LSCs remained two weeks after transplantation, suggesting that the cells were not engrafting permanently, as opposed to secreting factors for paracrine effects. Using a cytokine array, multiple proteins were identified in the LSC-conditioned media, including interleukin-6 (IL-6), insulin-like growth factor binding protein 2 (IGFBP-2), and hepatocyte growth factor (HGF), which are known to decrease inflammatory response among other effects. These results indicate that LSCs derived from healthy adult lung tissue can be produced using a simple, non-manipulative culture process and may provide regenerative therapeutic benefits in pulmonary fibrosis. Further studies will be required to elucidate the mode of action of LSCs *in vivo* to further understand the requirements for treating chronic lung diseases in humans.

© Copyright 2015 by Eric Thomas Henry

All Rights Reserved

Regenerative Potential of Adult Lung Spheroid Cells in a Bleomycin-Induced Pulmonary
Fibrosis Rodent Model

by

Eric Thomas Henry

A thesis submitted to the Graduate Faculty of
North Carolina State University
in partial fulfillment of the
requirements for the Degree of
Masters of Science

Biomedical Engineering

Raleigh, North Carolina

2015

APPROVED BY:

Dr. Ke Cheng
Committee Chair

Dr. Frances Ligler

Dr. Binil Starly

BIOGRAPHY

Eric Henry was born on February 6, 1991 in Raleigh, North Carolina to parents David and Melissa. He has three younger siblings, Bryan, Sarah, and Anna. Eric grew up in Apex, North Carolina, graduating from Apex High School in 2009. Eric attended North Carolina State University during undergraduate school, graduating in 2013 with a Bachelor's of Science in biomedical engineering. Throughout undergraduate school, Eric interned for multiple local biotechnology companies, including CRB consulting engineers, Medicago, and Pearl Therapeutics. Eric's education and employment opportunity led to an interest in innovative product design in the biomedical and pharmaceutical fields, prompting his interest in continuing his education at the graduate level. In 2013, Eric continued in the biomedical engineering program at NCSU and UNC pursuing a Masters of Science.

TABLE OF CONTENTS

LIST OF TABLES	vi
LIST OF FIGURES	vii
CHAPTER 1: INTRODUCTION AND LITERATURE REVIEW	1
1. Introduction.....	1
2. Background and Literature Review	1
2.1 Lung Anatomy	1
2.2 Lung Function and Measurement.....	3
2.3 Changes in Lung due to Chronic Pulmonary Disease	5
2.4 Current Treatment Standards for Chronic Lung Diseases.....	6
2.5 Stem Cell Therapy	8
2.6 Adult Lung Stem Cells	10
2.6.1 Alveolar Type II Cells	10
2.6.2 Club Cells and Bronchioalveolar Stem Cells.....	11
2.7 Culture Method for Stem Cell Production.....	11
2.8 In Vivo Model of Pulmonary Fibrosis.....	12
3. Objectives	13
CHAPTER 2: REGENERATIVE POTENTIAL OF ADULT LUNG SPHEROID CELLS IN A BLEOMYCIN-INDUCED PULMONARY FIBROSIS RODENT MODEL	14
1. Introduction.....	14
2. Materials and Methods.....	15

2.1	Cell Culture.....	15
2.2	Animal Procedures	16
2.2.1	Treatment of Severe Combined Immunodeficient Mouse Bleomycin-Induced Pulmonary Fibrosis Model with LSCs.....	17
2.2.2	Comparison of Syngeneic Rat MSC and Rat LSC Treatment of Wistar-Kyoto Rat Bleomycin-Induced Pulmonary Fibrosis Model	17
2.3	Histological analyses	17
2.3.1	Hematoxylin and Eosin (H&E) Staining	18
2.3.2	Masson’s Trichrome Staining.....	18
2.4	Flow Cytometry	18
2.5	Immunofluorescent Staining of Biomarker Antigens on Lung Spheroids and LSCs	19
2.6	In Vitro Assays of LSC-Conditioned Media	20
2.6.1	LSC-Conditioned Media Treatment of Bleomycin Injured Human Lung Epithelial Cells.....	20
2.6.2	Human Umbilical Vein Endothelial Cell Tube Formation Angiogenesis Assay	20
3.	Results.....	21
3.1	Proliferative Capacity of Lung Spheroid Cells.....	21
3.2	Characterization of Cell Phenotypes in Lung Spheroids and LSCs	23
3.3	Regenerative Effects of LSCs in a Murine Bleomycin-Induced Pulmonary Fibrosis Model	25

3.4	Comparison of Syngeneic Rat AD-MSCs and Rat LSCs in a Wistar-Kyoto Rat Model of Bleomycin-Induced Pulmonary Fibrosis.....	29
3.5	Potential Mechanism of LSC Therapeutic Benefit.....	30
4.	Discussion.....	32
CHAPTER 3: CONCLUSION AND FUTURE WORK.....		37
REFERENCES		38
APPENDICES		47
A.	Supplementary Figures	48
B.	Supplementary Tables.....	51

LIST OF TABLES

Supplementary Table 1- Lung donor information for the lung spheroid cells.....	51
Supplementary Table 2- List of antigenic markers used in analyses.....	52

LIST OF FIGURES

Figure 1-Gross anatomy of the human pulmonary system, including the upper airways, trachea, lungs and inset alveoli. [82]	2
Figure 2- Schematic of spheroid cell culture process, from tissue explant of the lung to Lung Spheroid Cells (LSCs).	15
Figure 3- Representative images of spheroid culture process at each step. I) Human lung tissue explant (right) with Explant Derived Cell (EDC) outgrowth, II) EDCs cultured in Ultra-low attachment flask spontaneously aggregate into lung spheroids, III) Lung spheroid plated in culture flask (center cell aggregate) with Lung Spheroid Cell (LSC) outgrowth, IV) LSCs expanded in culture near confluency.	21
Figure 4- Overall growth of LSCs in culture in Number of Doublings over Days. Each point represents a passage.	22
Figure 5- Immunofluorescent staining of lung spheroids. Top row: Lung spheroid including ATII (Pro-SP-C), Club cell (CCSP), and mesenchymal (CD90, CD105) markers; Bottom row: Hematopoietic markers (CD45, CD31, CD34). Pan cytokeratin is a marker for lung epithelial cells.	24
Figure 6- Top: Immunofluorescent staining of major LSC markers Pro-SP-C, CCSP, CD105, and CD90. Scale bars = 50 μ m. Bottom, left: Cell surface marker expression of various markers in positive percent when compared to iso controls. Bottom, right: Cytometric analysis of LSCs stained for Pro-SP-C and CCSP, top right quadrant represents dual positive. Data presented as mean \pm SD. N=3	25

Figure 7- Timeline of SCID murine pulmonary fibrosis model.	26
Figure 8- Comparison of groups in murine bleomycin induced pulmonary fibrosis model. Top row: Macroscopic view of sham, saline control, and LSC treated lungs. Second row: Hematoxylin and Eosin (H&E) stain of lung sections. Third row: Masson’s trichrome staining of lung sections. Bottom row, left: Quantification of Ashcroft scoring across the groups. Bottom row, right: Quantification of tissue infiltrates. All quantifiable results are based on the H&E stains. Data presented as Mean \pm S.D. Scale bars = 100 μ m. * indicates $p < 0.05$ when compared to the “Sham” group; # indicates $p < 0.05$ when compared to “Bleomycin + Saline” group. N= 6 – 7 animals per group.	27
Figure 9- Immunofluorescent staining of explanted murine lung. Top row: TUNEL staining of murine lung, including percent TUNEL positive quantification. Bottom row: Angiogenesis assay using vonWillebrands Factor to mark capillary structures. Data are presented as mean \pm SD. Scale bars = 20 μ m. * indicates $p < 0.05$ using unpaired Student’s t tests. N = 4 animals per group.	28
Figure 10- Comparison of groups (Left: Bleomycin + Saline Treatment; Middle: Bleomycin + AD-MSC treatment; Right: Bleomycin + LSC) in rat bleomycin induced pulmonary fibrosis model. Top row: Hematoxylin and Eosin (H&E) stain of lung sections. Bottom row, left: Quantification of Ashcroft scoring across the groups. Bottom row, right: Quantification of tissue infiltrates. All quantifiable results are based on the H&E stains. Data presented as Mean \pm S.D. Scale bars = 100 μ m. * indicates $p < 0.05$. N = 5 animals per group.	30

Figure 11- Left: Tube formation assay of LSC conditioned media versus control media on HUVEC cells cultured on Matrigel. Right: Live/dead assay of LSC conditioned media versus control media of cultured human lung epithelial cells. Data are reported as mean \pm S.D. Scale bars = 50 μ m. * indicates $p < 0.05$ when compared to control media group. N = 3 per group.	31
Supplementary Figure 1- Raw flow cytometry graphs for all analyzed markers vs. isotype control.....	48
Supplementary Figure 2- Immunofluorescence staining of cultured LSCs for multiple markers. Scale bar = 50 μ m.....	49
Supplementary Figure 3- Cytokine array showing presence of proteins in LSC conditioned media versus Normal Human Dermal Fibroblasts (NHDF).....	50

CHAPTER 1: INTRODUCTION AND LITERATURE REVIEW

1. Introduction

Chronic pulmonary diseases, such as emphysema and pulmonary fibrosis, lead to a decrease in lung function, which can be severely detrimental to the quality of life to patients suffering from these conditions. Many diseases increase the likelihood of acute complications, bacterial or viral infection and acute respiratory distress syndrome (ARDS) for instance, leading to drastic need for medical attention. Currently, treatments for chronic pulmonary diseases, while varied based on the specific condition of the patient, mainly consist of attempting to limit the symptoms causing decrease in quality of life. Generally, the treatment paradigm consists of various methods to decrease the impact of the disease depending on how far the progression of the particular condition has reached. The accepted treatment method for pulmonary fibrosis falls into this segmented category. Early pulmonary fibrosis therapies include pharmaceuticals to lessen the effects of the problematic symptoms. In later stages, doctors may include pulmonary rehabilitation and oxygen therapy. In the furthest progressed of cases, a full lung transplant may be attempted, but these have a very low success rate. Due to these difficulties, new treatments are required to battle pulmonary fibrosis.

2. Background and Literature Review

2.1 Lung Anatomy

The lungs are the major organ involved in the regulation of gases into and out of the body. Basically, the lungs are a series of tubes and cavities which act as the interface for gas transport. The pulmonary system includes the lungs, trachea, and overlaps a portion of the

circulatory system. As this research focuses on a specific disease state which mainly affects the lungs, the rest of the pulmonary system will only be described in brief (Figure 1).

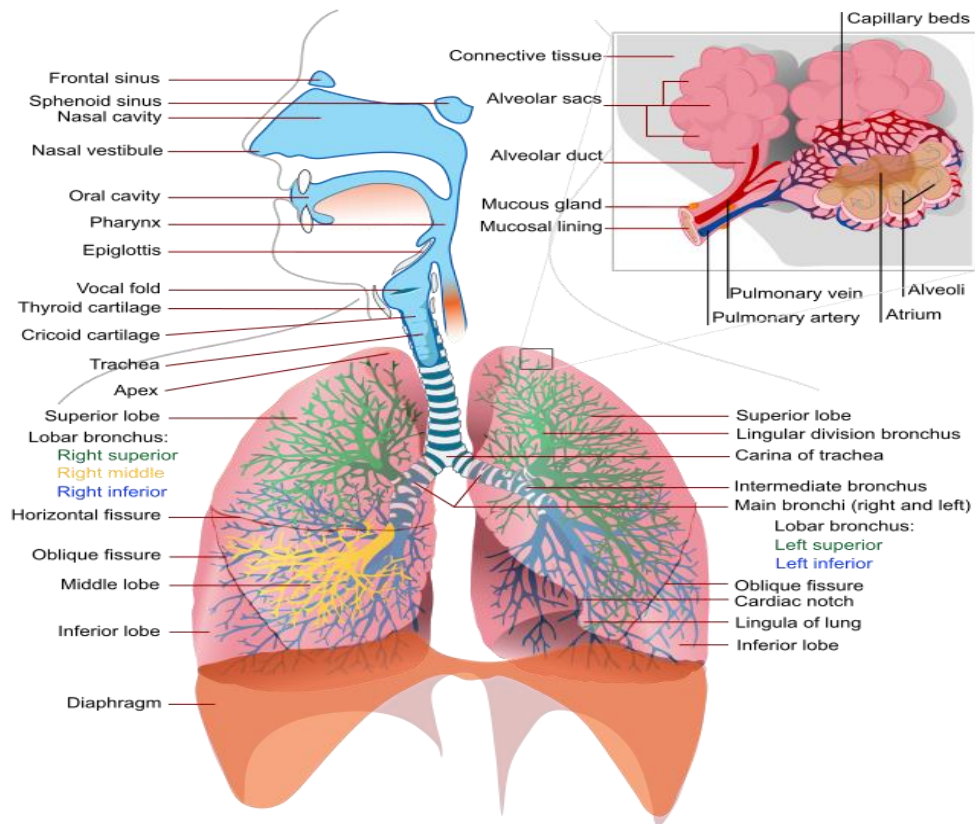


Figure 1-Gross anatomy of the human pulmonary system, including the upper airways, trachea, lungs and inset alveoli. [82]

The trachea is the cartilage-lined tube that connects the nasal and oral cavities to the lungs. Functionally, the trachea also acts as a filter and conditioning system to remove airborne particles and alter the humidity and temperature of the air before reaching the more sensitive lung tissue. The portion of the circulatory system that overlaps with the pulmonary system is the extensive capillary network which surrounds the lungs, allowing for gas exchange through diffusion across the lung walls. The lungs consist of a section of trachea referred to as a bronchi, which splits into smaller bronchioles throughout the lung. Each bronchiole ends in a collection of alveoli, the functional units of the lungs. The alveolar surface area is the boundary over which gas exchange occurs.

At the cellular level, the lung can be split into the airway and alveolar regions. The airways of the lung consist of multiple epithelial cell types (club cell, goblet cells, and ciliated cells), along with endothelial and matrix components [1]. Alveoli consist of alveolar type I and type II cells (ATI and ATII, respectively) in the epithelial layer and the endothelial layer consists of fibroblasts and a vast vasculature network [2], [3].

2.2 Lung Function and Measurement

As stated above, the main purpose of the lung is gas exchange: oxygen into the body and carbon dioxide out of the body. The transfer occurs through diffusion across the alveolar walls, specifically through the thin ATI cells. As air is taken into the lungs, the lungs expand, increasing the overall surface area of the alveoli. The ability of the lung to expand is also known as the lungs compliance. Also assisting in the compliance of the lung is a fluid secreted by the ATII called surfactant, which reduces surface tension across the alveoli. Changes in the

compliance, surfactant production, and the cells that exist in the lung can lead to diminished surface area, decreasing the gas exchange capability in some lung disease states such as pulmonary fibrosis or chronic obstructive pulmonary disease (COPD). In others, such as asthma, the lungs airways become restricted due to inflammation of the tissue. Clinically, these changes are measured through various volumes and pressures using spirometry, plethysmography, and pulse oximetry along with visual diagnoses through medical imaging techniques.

2.3 Changes in Lung due to Chronic Pulmonary Disease

While each chronic pulmonary disease leads to the decrease in gas exchange, the mechanism of damage is variable. A brief description of the major detrimental effect of multiple chronic and acute lung diseases follows in this section, with a focus on pulmonary fibrosis. The types of chronic lung disease can be separated categorically into three distinct, albeit not mutually exclusive, modes of action: inflammation, tissue destruction, or collection of fluid in the lung space. For diseases such as COPD and asthma, the airways of the lungs are inflamed, either constantly or under certain stimuli, respectively [4], [5]. Inflammation of the tissues in the lung can lead to tissue destruction, causing other conditions to arise, such as emphysema, the breakdown of the alveolar walls in the alveolar sac [6], [7]. Damage to the airway tissue can also be caused acutely, either through some form of infection or over-pressurization of the lung tissue. Depending on the severity of the damage in each acute case, it is possible to leave permanent scarring, thus creating a chronic disease. Fluid in the lungs includes both increased mucus production, as is seen in cystic fibrosis, or other bodily fluids (blood, water) leaking into the lungs, which is the case in pulmonary edema [8], [9]. The lungs of a patient who has pulmonary fibrosis will have an increase in fibrous or scar tissue in the airways and alveolar regions of the lungs. The fibrotic effects can have many causes, such as: environmental factors, radiation, chemical factors, or other disease states [10], [11]. There are also cases known as idiopathic pulmonary fibrosis, which have no known cause. What is understood about idiopathic pulmonary fibrosis, and pulmonary fibrosis of known cause, is that it is cyclic and progressive in nature. Once the tissue becomes scarred and inflamed, the

alveolar walls are thickened, leading to a cellular reaction which increases the production of growth factors linked to fibroblast production, therefore increasing the fibrogenesis and completing the cycle. [12].

2.4 Current Treatment Standards for Chronic Lung Diseases

Treating the various lung diseases described above can be a complex issue due to the high variability in symptoms that can arise in each case. Simply diagnosing the correct lung disease is difficult due to the amount of symptomatic overlap that can be seen clinically. In all of the chronic conditions there are no known cures as of yet so the treatment is simply to alleviate the severity of the symptoms and increase the overall quality of life. Another difficulty involved in treating chronic pulmonary diseases is that the disease can progress over time at a rate which is not known. While each disease affects the lungs through differing modes of action and there is a great deal of symptomatic overlap, the treatment regimens that are clinically prescribed for many chronic pulmonary conditions follow a similar structure. In the early stages of disease development all that is required for increasing the overall quality of life for the patient is normally to modify their environment and habits. As pulmonary fibrosis tends to arise later in the life, many of the patients who are diagnosed smoked for years, and quitting is the first habitual change that doctors recommend, along with other normal suggestions for leading a healthier lifestyle: losing weight, eating a more balanced diet, sleeping more regularly. By changing these factors, the progression of chronic lung diseases can be slowed. In the case where the symptoms cannot be diminished through simple lifestyle changes, there are multiple pharmaceuticals that can be applied depending the each patient's scenario. As

most of the pulmonary diseases are caused by or lead to inflammatory responses in the lung tissue, the normal first step is the prescription of a corticosteroid, such as prednisone or budesonide [13]–[16]. Reducing the inflammatory response can lead in a decrease in airway constriction and less damage done over time to the lungs, slowing the progression of the disease. Recently, two new drugs have been approved by the FDA for use in treating pulmonary fibrosis, Ofev (nintedanib) and Esbriet (pirfenidone) [17]. Nintedanib is a commonly used non-small cell lung cancer treatment for decreasing angiogenesis in tumor growths [18]. Nintedanib has been shown in multiple clinical trials to be safe and effective at treating pulmonary fibrosis, by blocking multiple known pathways involved in the progression of the disease [19]–[22]. Pirfenidone is used as an anti-fibrotic agent, which functions by reducing fibroblast proliferation, which limits collagen deposition in the lungs [23]–[26]. While the combination of Ofev and Esbriet shows promise in limiting the progression of pulmonary fibrosis, there is still no cure, or treatment shown to reverse the effects of the disease. Due to the lack of current options for patients suffering from pulmonary fibrosis, the aforementioned pharmaceuticals will quickly become the new gold standard for treating this disease, although there are risks involved due to side-effects of the medication. Both Ofev and Esbriet result in modifications in liver function, which requires monitoring [27]. Due to nintedanib's mechanism of decreasing angiogenesis, the wound healing process can also be disrupted, which also requires monitoring [19]. In the more severe cases, oxygen therapy is used to increase the environmental oxygen to the lungs to make up for the lungs inability to perform normally. While effective, this provides no therapeutic benefit for the chronic

condition causing the diminished capacity. For the most severe cases, the final effort is a full lung transplant. The success rate for a lung transplant in a patient suffering from idiopathic pulmonary fibrosis is approximately 45% for the first five years [28]. Current research is being performed to develop more effective biological therapies to attempt to reverse the effects of chronic lung diseases along with therapies that prohibit the continued damage to the lungs.

2.5 Stem Cell Therapy

Throughout the medical landscape, the use of stem cells as a treatment method has become a hotbed for research and clinical progress. The power driving stem cell therapeutics is the ability of the treatment cell to differentiate down a controlled pathway in order to provide either physical replacement of a damaged tissue or provide chemical signals to induce the body to repair the tissue and alleviate the condition. Stem cells can undergo self-renewal and asymmetric division. There are two main categories of stem cells that are used in preclinical and clinical research today: pluripotent stem cells (e.g. embryonic stem cells [ESCs] and induced pluripotent stem cells [iPSCs]) and multipotent stem cells (including mesenchymal stem cells [MSCs] and organ-specific adult stem cells). The highest potency stem cell tested in clinical trials is the induced pluripotent stem cell, not including embryonic stem cells due to the ethical landscape that limits the clinical applicability. iPSCs are differentiated adult cells which have been genetically modified to revert back to an undifferentiated state [29], [30]. By following specific protocols, such as the ones described in Yan et al., Liu et al., and Zhang et al., it is possible to then lead iPSCs down a specific differentiation pathway to a desired cell phenotype [30]–[32]. The drawback with iPSCs is the difficulty involved in controlling the

differentiation outside of a research setting. In studies using iPSCs, it has been shown that under the incorrect conditions, the risk for teratogenesis increases [33]–[36]. With the increase in risk, the amount of regulations placed on any potential product using iPSCs drastically lengthens the time and increases the cost of clinical trials, leading to almost no clinical trials being completed using iPSCs [36], [37]. MSCs are less potent than iPSCs, although MSCs are still more multi-potent than organ-specific adult stem cells. MSCs can be derived from multiple sources in the body, in many cases bone marrow [BM-MSCs] and adipose tissue [AD-MSCs], and are easily obtained in comparison to either of the other two stem cell categories [38]–[40]. Like iPSCs, MSCs also include the risk of tumor promotion, although not at the scale that iPSCs have been shown to exhibit, which is why MSCs are so commonly used in thousands of clinical trials in the United States today [41]. In contrast to both iPSCs and MSCs, adult stem cells are normally uni-potent, only able to differentiate further into an already specified tissue type. Adult stem cells are found within the organ in localized niches. While less popular in use than MSCs, adult stem cells have been shown to be an effective treatment in clinical trials [42]–[44]. Due to the nature of adult stem cells, the teratogenic risk is diminished in contrast to the other stem cell types, leading to a less stringent regulatory path. While the lessened risk assists in convincing regulatory bodies to allow this form of treatment, adult stem cells are complicated to produce due to either a lack of knowledge about the specific cell type for the tissue or difficulty in production of large enough cell quantities.

2.6 Adult Lung Stem Cells

As stated previously, adult stem cells can be difficult to determine for a particular organ, especially the lung. Since the discovery of localized niches of stem cells dedicated to the renewal of specific organs, there has been research into elucidating a population of cells within each organ that function as the progenitors for local repair [45], [46]. In some organs, such as the skin and intestines, the region housing the stem cell niche has already been identified [47]–[50]. In the adult lung, the local stem cell populations were not discovered until the mid-2000s, when certain cell types within the lung were shown to fit the requirements described above to be a stem cell [1], [3], [51].

2.6.1 Alveolar Type II Cells

The alveoli, as described above, mainly consist of alveolar type I [ATI] and alveolar type II [ATII] cells. The ATI cells are terminally differentiated epithelial cells that cover the majority of the surface area of the lung and are characterized by the expression of Aquaporin 5 [Aq5] [52], [53]. The ATII cells, however, are non-terminal cells, which have been shown to act as progenitor cells for the alveoli. According to research by Barkauskas et al., ATII cells were able to both self-renew over extended periods of time and recapitulate the alveolar environment including generate ATI cells when cultured with stromal signaling cells [3]. Functionally, ATII cells also secrete proteins, such as surfactant, which acts to assist the lung in compliance. Phenotypically, ATII cells express prosurfactant protein C (Pro-SP-C) which is not expressed in the differentiated ATI state [53], [54]. This antigenic marker is used in the research to distinguish between these two main cell populations.

2.6.2 Club Cells and Bronchioalveolar Stem Cells

The cell that acts as the progenitor for the bronchioles is the club cell [1], [55]. Within the bronchioles, the non-differentiating club cell functions similarly to the ATII cells described above, secreting proteins, specifically uteroglobin, along with detoxifying material that has been inhaled into the lungs [56]. During normal cellular repair, club cells can self-renew and differentiate into ciliated cells [55]–[57]. Bronchioalveolar stem cells have been identified as a separate subgroup between the club and ATII cells, specifically focused on regeneration of the bronchioalveolar duct, which express both ATII and club cell markers [1].

2.7 Culture Method for Stem Cell Production

When treating any condition using a stem cell or stem cell-based therapeutic, there are two main hurdles which must be overcome during product development for the treatment to be a viable venture: 1. the amount of cells required for a dose and the technology for producing that number of cells, and 2. clear safety tests which show minimal risk. Without both of these criteria being met, the product will never exit research stage trials. To deal with the acquisition of stem cells which are not readily available, many clinical trials use MSCs and a great deal of research work is being done on iPSCs. As stated above, these cell types have some inherent teratogenic risk which leads to safety issues. For iPSCs there is also a need for genetic modification of the cells [29], [30]. In MSC trials, some protocols require the addition of factors or other cell types to manipulate the cells a certain way before they can be used as a treatment. Any manipulation of the cells leads to a more difficult regulatory pathway, increasing the cost of the potential trials. Manipulations are also difficult to translate to a large

scale. One culture method that has previously been shown to be viable in multiple organ systems, including neural and cardiac tissue, is the multi-cellular spheroid culture system [58]–[61]. This method, described in detail in the Materials and Methods section below, includes the use of monolayer proliferation and three-dimensional suspension culture selection. This system includes only basic culture steps such as passaging and use of basic growth media. When used with autologous cells, the spheroid culture method greatly reduces the risk of negative modifications to the cells and fits within the simpler regulatory path.

2.8 In Vivo Model of Pulmonary Fibrosis

To study the effects of cellular therapies in pulmonary fibrosis, an animal model is required for the study. One common model of pulmonary fibrosis involves the administration of bleomycin, an antitumor antibiotic, either intravenously or intratracheally [62]–[64]. The amount of bleomycin administered is based on the method of injection. In intravenous models, which are more commonly used for damage over time, the amount of bleomycin is heightened per injection, between 100-200 U/kg of body weight, but daily injections are required for continued damage [63]. Intratracheal injection of bleomycin is more directly damaging as it comes in direct contact with the epithelial of the lungs, leading to a single, smaller dose required, between 0.5-7.5 U/kg [62], [65]. The injury model used in this research is the acute intratracheal instillation to limit the requirement for surgical intervention and anesthetic use. Due to the nature of the treatment, the model to be used requires a compromised immune system to avoid rejection of the injected LSCs. Severe combined immunodeficient (SCID) mice are therefore used to circumvent immune response leading to

unexpected variations in results [66]. For the syngeneic comparison of rat AD-MSCs and LSCs described below, Wistar-Kyoto rats were used as opposed to SCID mice, as the immune response is negligible based on the genetic similarity of the individual rats.

3. Objectives

This thesis study aims to verify that the spheroid culture process described above is an applicable method for the generation of lung progenitor cells. The product cells (lung spheroid cells, LSCs) will then be characterized to identify the phenotypic expression in relation to previous data. If the LSCs include previously described lung progenitor cells, a rodent model of pulmonary fibrosis will be used to define their regenerative potential *in vivo* along with *in vitro* verification assays.

CHAPTER 2: REGENERATIVE POTENTIAL OF ADULT LUNG SPHEROID CELLS IN A BLEOMYCIN-INDUCED PULMONARY FIBROSIS RODENT MODEL

1. Introduction

As described above, a more effective treatment option for pulmonary fibrosis is needed that limits the risks of negative side effects and is simple to manufacture robust and clinically viable fashion. Stem cell-based biologics have shown promise recently for providing therapeutic effects in lung disease animal models, along with some early clinical trials in human patients. Currently, the clinical focus is on the use of mesenchymal stem cells for treating chronic disease, although these cells require more direct control over the desired differentiation pathway along with potential for minor teratogenic risk. While a more effective treatment of a currently incurable condition greatly outweighs the limited risks involved, reducing the risk factors through a non-mesenchymal stem cell would foster a more streamlined regulation process.

The research presented below aims to describe the simple production and therapeutic benefit of human adult lung-derived progenitor cells, based on the spheroid culture method used in previous research [43], [59], [67]. These Lung Spheroid Cells (LSCs) were cultured and used for characterization and verification of clinical potential through *in vitro* and *in vivo* experimental assays.

The results described in this chapter are summarized in a manuscript which is currently under revision in *Stem Cells: Translational Medicine* with co-authors: M. Taylor Hensley, Jhon Cores, Shirena Anthony, Adam Vandergriff, James B.M. de Andrade, Tyler Allen, Thomas G. Caranasos, L. Jason Lobo, and Ke Cheng.

2. Materials and Methods

2.1 Cell Culture

Normal human distal lung tissue samples (n=4) were acquired from the University of North Carolina-Chapel Hill Cystic Fibrosis/Pulmonary Research and Treatment Center. All explant samples were from healthy, non-smoking donors. Explants were processed in accordance with previously described protocols from Li et al. and Makkar et al [42], [68] (Figure 2).

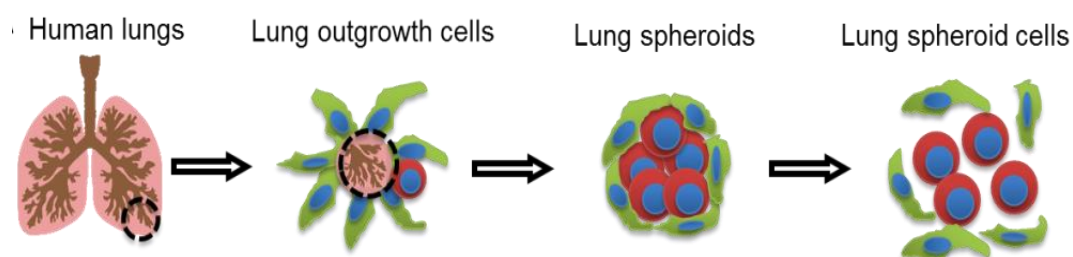


Figure 2- Schematic of spheroid cell culture process, from tissue explant of the lung to Lung Spheroid Cells (LSCs).

Briefly, explant sections similarly sized to a lung biopsy were taken from the distal lung section obtained and sliced into smaller sections. These sections were then washed with phosphate-buffered saline (PBS, Gibco, 10010-023) and incubated for 5 minutes in collagenase solution (Sigma, C1889). After incubation, culture medium containing 20% Fetal Bovine Serum (FBS, Sigma, F0926) was added to neutralize the digestive process. The explant sections were then minced into smaller pieces, approximately 0.5 mm in diameter and plated onto fibronectin (Fisher, cv40008b) coated 150 mm² dishes with 7 mL of culture media, separated by approximately 10 mm between each sample. The dishes were then incubated at 37 C overnight. The next day 10 mL of culture media was added to the dish. From this point, the dishes were observed and media changed (30 mL) every 2-3 days until the outgrowth cells reach contact confluency between individual explants (approximately 16 days). Once confluency was reached, the cells were detached from the dish using Tryple Select (Gibco, 12563-029). The cells harvested from the explants are the Explant Derived Cells (EDCs). EDCs were then cultured in suspension in Ultra-Low Attachment flasks (Sigma, CLS3814) with 10% FBS culture media for 6 days to create cellular spheroids. The spheroids were then removed and plated back onto tissue culture flasks coated with fibronectin. Plated spheroids outgrow into LSCs which were then used for further experimentation.

2.2 Animal Procedures

All animal work is compliant with the Institutional Animal Care and Usage Committee at North Carolina State University (IACUC #13-128-B). Multiple animal studies were performed and described.

2.2.1 Treatment of Severe Combined Immunodeficient Mouse Bleomycin-Induced Pulmonary Fibrosis Model with LSCs

Severe Combined Immunodeficient (SCID) mice (Charles River Laboratories, strain 236, female, 6-8 weeks old) were randomly separated into three different groups (n=6 or 7 per group): sham, PBS control, LSC treatment. All groups underwent surgical intratracheal injections with the sham group receiving 50 μ L PBS and the PBS control and LSC treatment receiving 0.7U/kg bleomycin (CalBiochem, 203401) in 50 μ L PBS. Twenty-four hours after injury, treatment was provided through tail vein injection of either 200 μ L PBS for the sham and PBS control groups or 1×10^6 human LSCs in 200 μ L PBS for LSC treatment group. All mice were then monitored for 13 days before being sacrificed for analysis.

2.2.2 Comparison of Syngeneic Rat MSC and Rat LSC Treatment of Wistar-Kyoto Rat Bleomycin-Induced Pulmonary Fibrosis Model

Wistar-Kyoto Rats (Charles River Laboratories, strain 008, female, 6 weeks old) were randomly separated into three groups (PBS, n=5; AD-MS, n=5; LSC, n=5). All rats underwent intratracheal instillation of 0.7 U/kg bleomycin in 200 μ L of PBS. Twenty-four hours after injury, treatment was provided through an intravenous injection of PBS, 5×10^6 MSCs or LSCs suspended in 350 μ L. All rats were then monitored for 14 days before being sacrificed for identical analysis to the SCID mice.

2.3 Histological analyses

As stated in the animal procedures above, all animals were sacrificed 14 days post bleomycin injury for analysis. Animal lungs were harvested, washed in PBS, and processed

through 0-30% sucrose solutions in PBS to preserve the tissue integrity of the lung. The processed lungs were then frozen in Optimum Cutting Temperature Compound (OCT Compound, Tissue-Tek, 4583). The frozen lungs were then cryosectioned into 5 μm thick sections for use in multiple analytical methods.

2.3.1 Hematoxylin and Eosin (H&E) Staining

Microscope slides with cryosections attached were processed through a standard Hematoxylin and Eosin (H&E) staining procedure [54]. Simply, the staining procedure includes a series of washes which color various cellular components either blue (Hematoxylin) or red (Eosin). H&E stained lung sections were imaged using (microscope info). The images acquired were quantitatively analyzed through Ashcroft scoring and infiltration measurement [54], [69]. Analyses were performed blind as to avoid investigator bias.

2.3.2 Masson's Trichrome Staining

Microscope slides with cryosections attached were processed through a standard Trichrome staining procedure [69]. Trichrome staining is very similar to H&E, with various cellular components being stained either blue, dark red, or pink. Masson's is useful in its separation of the non-nuclei portions of cells and the extracellular spaces, allowing for connective tissue and matrix visualization.

2.4 Flow Cytometry

Flow cytometry was performed to verify the antigenic phenotype of the LSCs. The cells were cultured normally until confluency. Once confluent the cells were harvested, separated into 0.25×10^6 vials for each marker, and washed in MACS Flow Buffer (MACS Miltenyi

Biotec, 130-091-222). Between each wash the vials were centrifuged at 1700rpm for five minutes to pellet the cells. After two washes, the flow buffer was removed and the cells were either: (1) incubated at 4°C in the dark with a labelled antibody for one hour, (2) incubated at 4°C in the dark with an unlabeled antibody for one hour, or (3) incubated at 4°C in fixation/permeabilization solution for 20 minutes (BD, 554714); depending on which biomarker was targeted for identification. In case (1), once the incubation was complete, the cells were washed twice in Flow Buffer before being analyzed. In case (2), the sample incubated with unlabeled antibody was washed in flow buffer twice before incubating with a fluorescent anti-Ig antibody. In case (3) the cells either follow the case (1) or (2) procedure with the flow buffer washes replaced with fixation/permeabilization solution washes. Isotype-identical species-matched antibodies served as negative controls. For a full list of antibody markers see appendix B, supplementary table 2. Cytometric analysis was performed using either a FACSCalibur or LSR II Flow Cytometer (BD) and analyzed using FlowJo analysis software (FlowJo, LLC).

2.5 Immunofluorescent Staining of Biomarker Antigens on Lung Spheroids and LSCs

For immunofluorescence staining of LSCs, the cells were cultured on fibronectin-coated chamber slides. Slides with confluent cells were washed with PBS and fixed with 4% paraformaldehyde (PFA) for 30 minutes (Alfa Aesar, 43368). After fixation, the cells were washed and permeabilized with DAKO Protein block containing 0.1% saponin for one hour at 4°C (DAKO Protein Block: Dako, X0909; Saponin: Sigma, 47036). Following permeabilization, the cells were incubated with antibody diluted in DAKO block at 4°C in the

dark overnight. The cells were washed the next day with PBS and then incubated with a secondary fluorescent antibody for 1.5 hours at room temperature, before washing and staining the nuclei with DAPI in PBS for 10 minutes at room temperature (Life Technologies, R37606). The fully stained cells were washed and mounted with Prolong Gold (Life Technologies, P36930) for viewing. Staining of the lung spheroids followed the same protocol, but required the spheres to be cryosectioned at 5 μm after mounting in Optimum Cutting Temperature (OCT) compound before the immunofluorescence procedure can be initiated.

2.6 In Vitro Assays of LSC-Conditioned Media

LSCs were cultured following the above culture protocol. Once confluent, the LSCs were then washed with PBS and cultured with IMDM for three days. The resulting media was collected and used for analysis of LSC-conditioned media.

2.6.1 LSC-Conditioned Media Treatment of Bleomycin Injured Human Lung Epithelial Cells

Human Lung Epithelial Cells (HLECs) were cultured using 20% FBS growth media. Once the cells attached and reached approximately 60% confluency, the growth media was removed and PBS containing bleomycin was introduced to the culture to damage the cells. The damaged cells were then treated with control media or LSC-conditioned media and cell death was observed with a Calcein-AM Live/Dead assay.

2.6.2 Human Umbilical Vein Endothelial Cell Tube Formation Angiogenesis Assay

The angiogenic effect of LSC-conditioned media was analyzed using the endothelial tube formation assay [70], [71]. In brief, a basement membrane compound, in this case MatrigelTM was used as a three dimensional construct to culture human umbilical vein

endothelial cells (HUVECs). During the culture process, either control media or LSC-conditioned media was applied to the cells. When cultured on a basement membrane compound, endothelial cells tend to create tube-like structures which is indicative of angiogenesis [70], [71]. After culturing with the control and LSC-conditioned media, the tube formation was analyzed for number of tubes and length of tubes formed.

3. Results

3.1 Proliferative Capacity of Lung Spheroid Cells

Human lung explants were acquired and cultured using a common three-dimensional culture method described above[42], [43]. During the explant stage, multiple cell types can be seen outgrowing from the plated explant tissue (Figure 3).

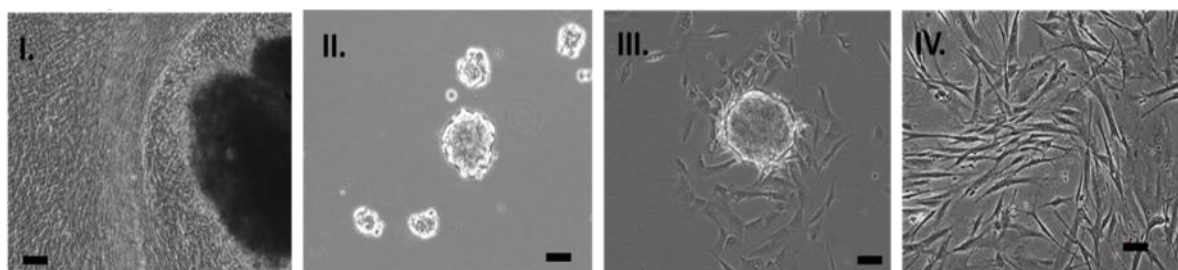


Figure 3- Representative images of spheroid culture process at each step. I) Human lung tissue explant (right) with Explant Derived Cell (EDC) outgrowth, II) EDCs cultured in Ultra-low attachment flask spontaneously aggregate into lung spheroids, III) Lung spheroid plated in culture flask (center cell aggregate) with Lung Spheroid Cell (LSC) outgrowth, IV) LSCs expanded in culture near confluency.

Explant outgrowth confluency takes approximately sixteen days, at which point the cells (10-20 million) were harvested and re-cultured in Ultra-Low Attachment flasks for suspension

culture [72], [73]. Seeding the cells in the suspension culture encourages the explant derived cells to form spheroids spontaneously (Figure 3-II). After approximately six days, the majority of the explant-derived cells aggregated into spheroids and were re-cultured in adherent culture in a fibronectin-coated flask. The spheroids attach to the surface of the flask, and the lung spheroid cells grew out from the three-dimensional conglomerate (Figure 3-III). LSCs maintain proliferative capacity and visual consistency until approximately passage seven, with a passage occurring every three-to-seven days post seeding (Figure 4). Overall, from a single biopsy, up to 15 doublings were recorded in approximately 50 days (Figure 4). For further translation into the clinical setting, this yield would be sufficient for an autologous treatment regimen, based on the cell yields used in current MSC dosing in clinical trials varying between 20-200 million cells [74], [75].

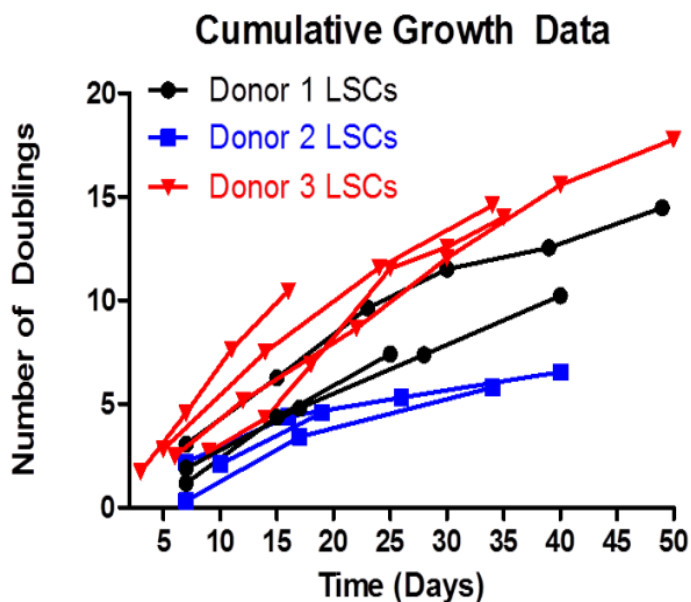


Figure 4- Overall growth of LSCs in culture in Number of Doublings over Days. Each point represents a passage.

3.2 Characterization of Cell Phenotypes in Lung Spheroids and LSCs

Describing the antigenic phenotype of lung spheroids and LSCs was done through immunofluorescence staining and flow cytometric analysis (only in LSCs). For more detailed results of the biomarker studies, see (Supplementary Figures 1-2); selected results from the characterization protocols will be reported on in this section. Lung spheroids showed spontaneous three-dimensional organization into self-contained cellular environments. The internal cellular makeup of the spheroids showed an increased amount of lung progenitor markers Pro-SP-C and CCSP, which correspond to known alveolar and airway stem cells, ATIIs and club cells, respectively, residing in the center of the sphere, while cells expressing known mesenchymal markers, CD90 and CD105, populated mainly the outer surface of the sphere (Figure 5 top). Staining for non-lung markers, CD31, CD34, and CD45 showed that the lung spheroid method did not include the hematopoietic cells that are commonly used in other research, such as bone marrow mesenchymal stem cells (Figure 5 bottom) [76]–[78].

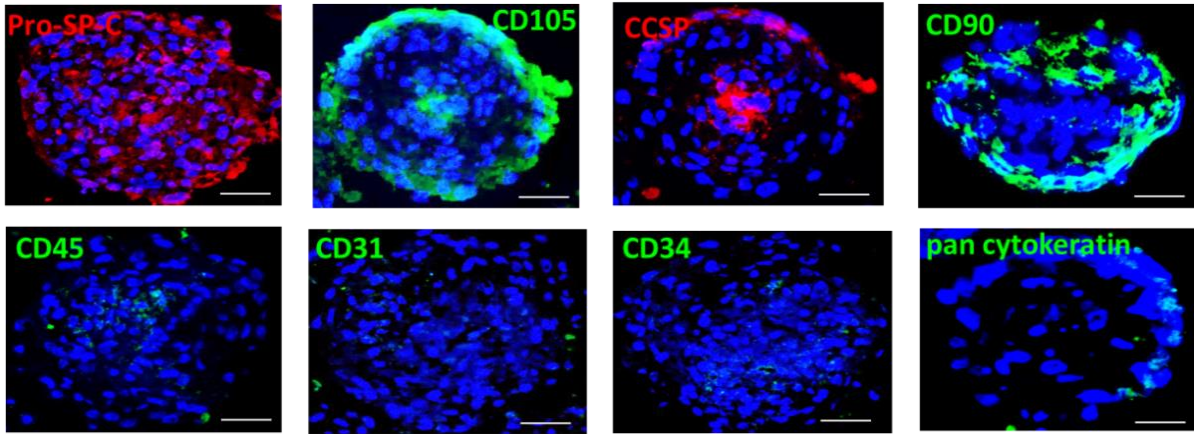


Figure 5- Immunofluorescent staining of lung spheroids. Top row: Lung spheroid including ATII (Pro-SP-C), Club cell (CCSP), and mesenchymal (CD90, CD105) markers; Bottom row: Hematopoietic markers (CD45, CD31, CD34). Pan cytokeratin is a marker for lung epithelial cells.

LSCs showed similar results in regards to immunofluorescence staining and cytometric analysis verified the results numerically (Figure 6).

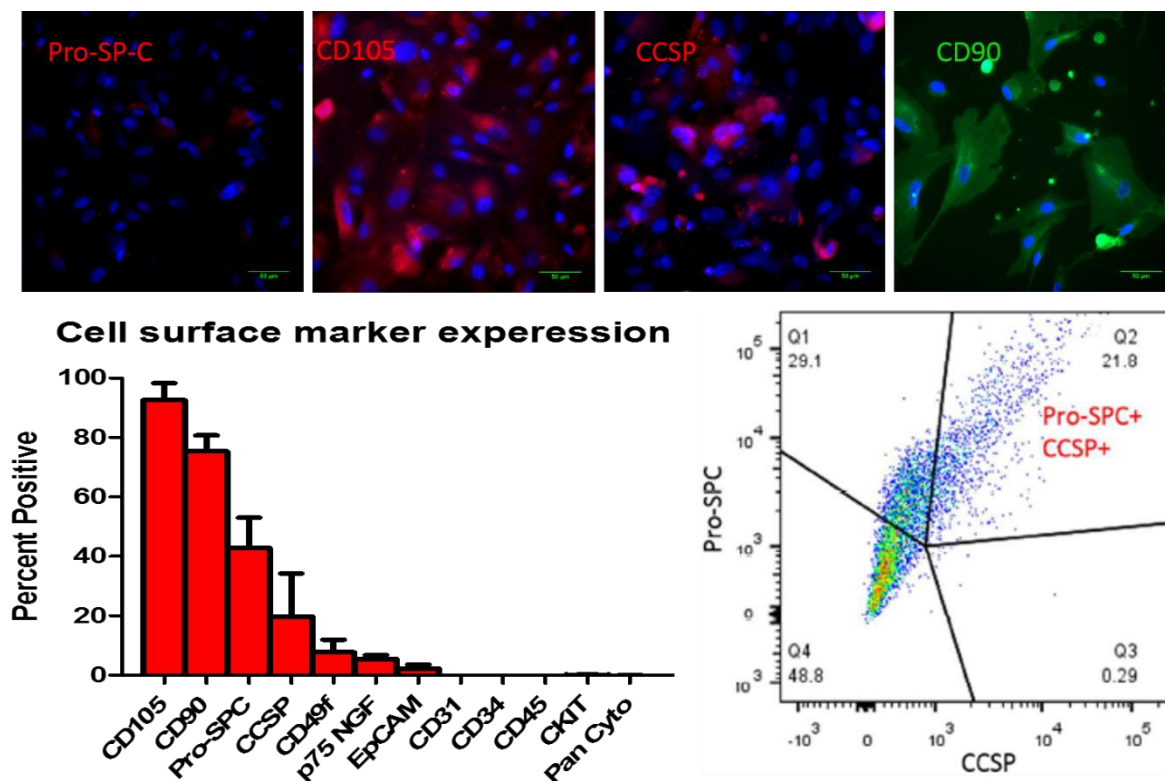


Figure 6- Top: Immunofluorescent staining of major LSC markers Pro-SP-C, CCSP, CD105, and CD90. Scale bars = 50 μ m. Bottom, left: Cell surface marker expression of various markers in positive percent when compared to iso controls. Bottom, right: Cytometric analysis of LSCs stained for Pro-SP-C and CCSP, top right quadrant represents dual positive. Data presented as mean \pm SD. N=3

3.3 Regenerative Effects of LSCs in a Murine Bleomycin-Induced Pulmonary Fibrosis Model

A severe combined immunodeficient (SCID) mouse model with bleomycin-induced pulmonary fibrosis was used as an *in vivo* method of testing the efficacy of LSCs as a treatment in pulmonary fibrosis. A study outline and timeline is provided (Figure 7).

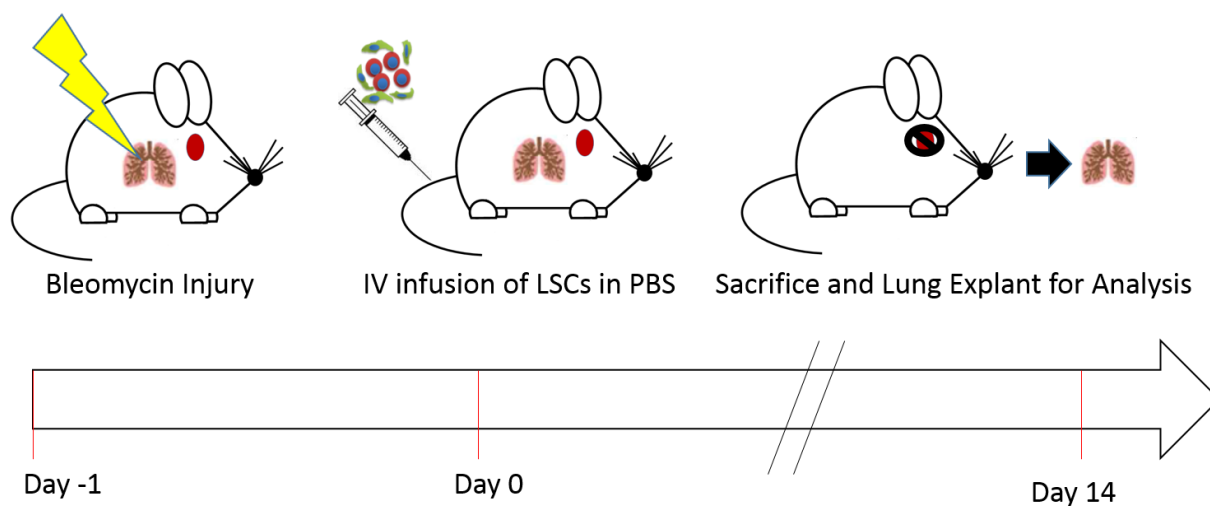


Figure 7- Timeline of SCID murine pulmonary fibrosis model.

Analysis of the lungs *ex vivo* was performed after sacrifice through histological and immunofluorescence staining. Tissue damage was visible macroscopically on the outside of the damaged lungs treated with saline in comparison to the sham and LSC treated group (Figure 8, top row). Histological staining with H&E and Masson's Trichrome both showed fibrotic tissue decrease in the treatment groups, as measured through the Ashcroft method (Figure 8, 2nd-4th row) [69]. A tissue infiltrate count verified the Ashcroft results (Figure 8, bottom row).

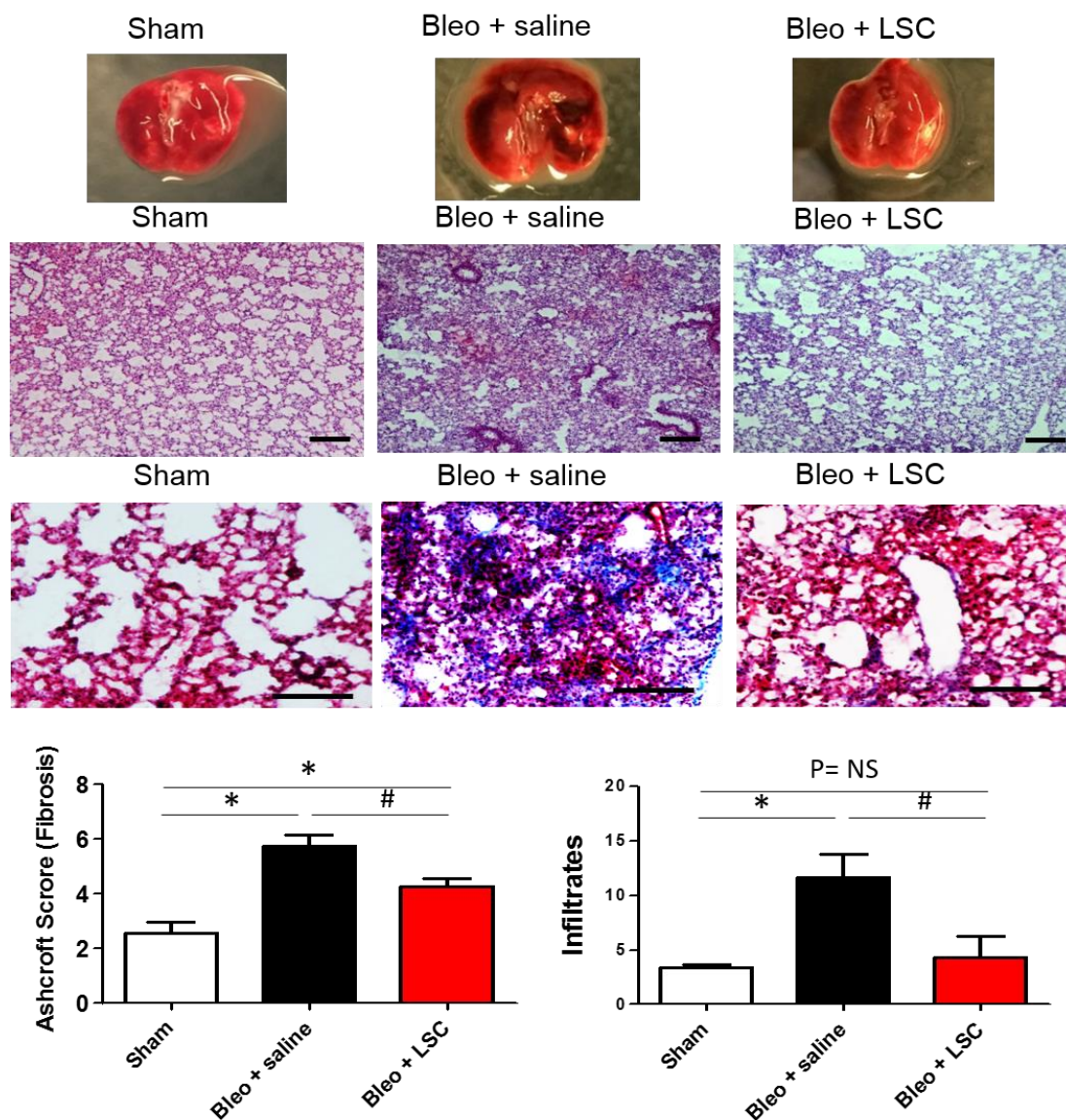


Figure 8- Comparison of groups in murine bleomycin induced pulmonary fibrosis model. Top row: Macroscopic view of sham, saline control, and LSC treated lungs. Second row: Hematoxylin and Eosin (H&E) stain of lung sections. Third row: Masson's trichrome staining of lung sections. Bottom row, left: Quantification of Ashcroft scoring across the groups. Bottom row, right: Quantification of tissue infiltrates. All quantifiable results are based on the H&E stains. Data presented as Mean \pm S.D. Scale bars = 100 μ m. * indicates $p < 0.05$ when compared to the "Sham" group; # indicates $p < 0.05$ when compared to "Bleomycin + Saline" group. N= 6 – 7 animals per group.

A terminal deoxynucleotidyl transferase dUTP nick end labeling [TUNEL] assay was performed to compare apoptotic cell numbers (Figure 9, top). Fewer apoptotic cells were evident in regions with LSC engraftment in comparison to regions within the same lung without LSC engraftment. Along with decreased apoptosis, the LSC-treated group showed an increase in angiogenesis. Staining for von Willebrands Factor (vWF) exhibited a higher capillary density in the LSC-treated lungs in comparison to saline controls, which indicates an increase a promotion of new vascularization or the inhibition of vascular degeneration after injury. (Figure 9, bottom).

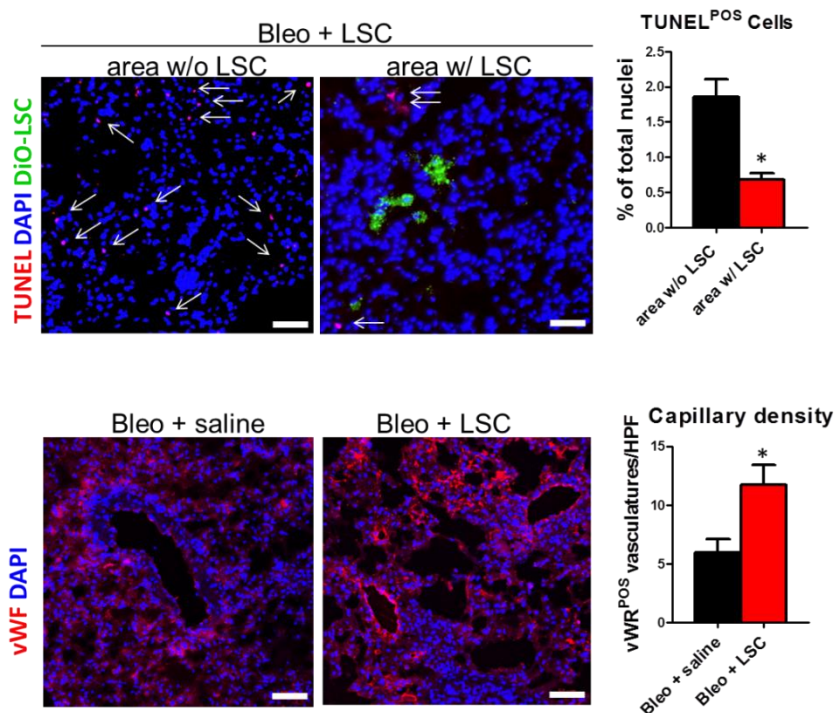


Figure 9- Immunofluorescent staining of explanted murine lung. Top row: TUNEL staining of murine lung, including percent TUNEL positive quantification. Bottom row: Angiogenesis assay using vonWillebrands Factor to mark capillary structures. Data are presented as mean \pm SD. Scale bars = 20 μ m. * indicates $p < 0.05$ using unpaired Student's t tests. N = 4 animals per group.

3.4 Comparison of Syngeneic Rat AD-MSCs and Rat LSCs in a Wistar-Kyoto Rat Model of Bleomycin-Induced Pulmonary Fibrosis

For comparison of syngeneic MSCs and LSCs, a Wistar-Kyoto pulmonary fibrosis model was used. After sacrifice, the rat lungs were harvested and analyzed following the same techniques used in the SCID mouse analysis. Histological analysis and quantification revealed that both AD-MSCs and LSCs decrease the overall fibrotic effect of bleomycin on the lungs, while the LSCs decreased the fibrotic score and tissue infiltrates measurement significantly more than the AD-MSCs (Figure 10).

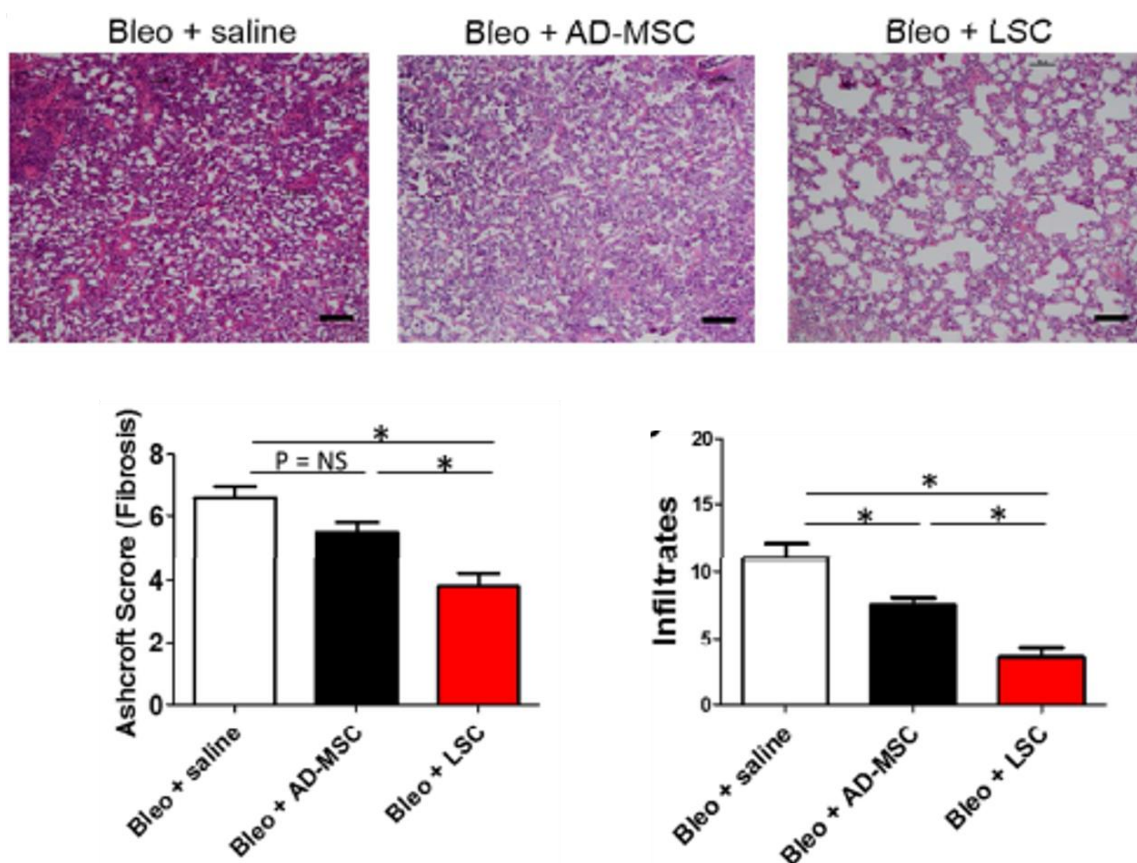


Figure 10- Comparison of groups (Left: Bleomycin + Saline Treatment; Middle: Bleomycin + AD-MSC treatment; Right: Bleomycin + LSC) in rat bleomycin induced pulmonary fibrosis model. Top row: Hematoxylin and Eosin (H&E) stain of lung sections. Bottom row, left: Quantification of Ashcroft scoring across the groups. Bottom row, right: Quantification of tissue infiltrates. All quantifiable results are based on the H&E stains. Data presented as Mean \pm S.D. Scale bars = 100 μ m. * indicates $p < 0.05$. N = 5 animals per group.

3.5 Potential Mechanism of LSC Therapeutic Benefit

While there is some engraftment of the injected LSCs into the treated lung, the amount of engraftment does not necessarily indicate that the injected cells are reconstructing the damaged lung tissue (Figure 9, top, DiO labeled). Instead, it was found that the cells were relatively diminished in the lungs at the end of the two weeks. This being the case, it is more

likely that the injected LSCs are functioning by secreting factors into the cellular system reducing the effects of the bleomycin. A tube formation and live/dead assay was run to further verify the effects of LSC conditioned media on human lung endothelial and epithelial cells, respectively (Figure 12).

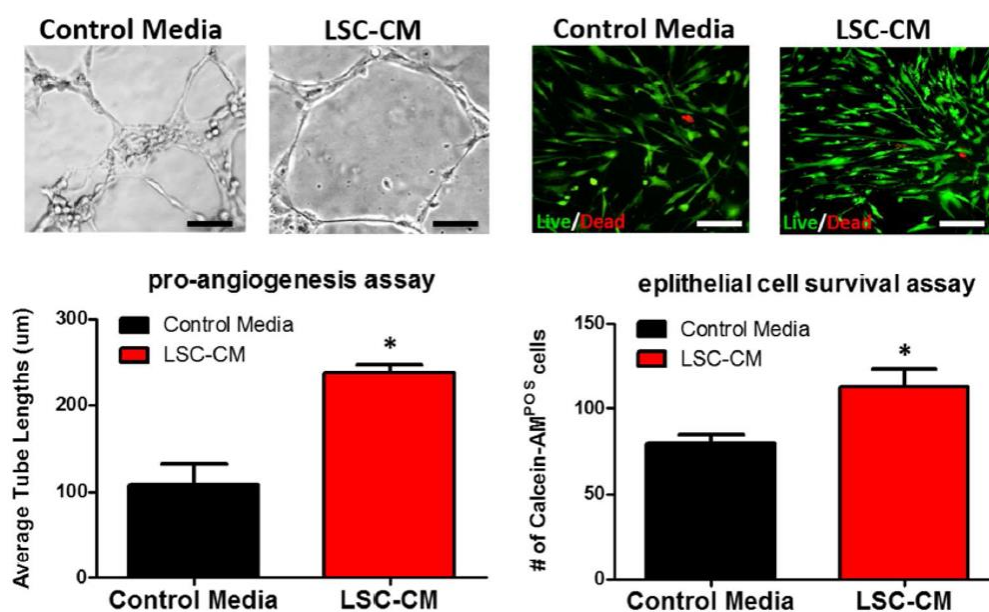


Figure 111- Left: Tube formation assay of LSC conditioned media versus control media on HUVEC cells cultured on Matrigel. Right: Live/dead assay of LSC conditioned media versus control media of cultured human lung epithelial cells. Data are reported as mean \pm S.D. Scale bars = 50 μ m. * indicates $p < 0.05$ when compared to control media group. N = 3 per group.

4. Discussion

Stem cell therapies for diseases which are difficult to treat using traditional methods have garnered a significant amount of attention in the clinical research community recently. Thousands of clinical research trials on the effects of stem cells are underway in the United States alone, although few products have been approved for market use [17], [19], [24]. The vast majority of the current clinical trials use mesenchymal stem cells due to the ease of acquisition and known origin of cell source. A separate, potentially more applicable cell source is the organ specific adult stem cells. In the lungs, the local stem cells are the alveolar type II, club, and bronchioalveolar cells [1]–[3]. These cell types can be used as a stem cell population for the treatment of chronic pulmonary diseases. The research presented in this thesis covers the generation, characterization, and use of the isolated and expanded stem cell populations as a treatment in an *in vivo* model of pulmonary fibrosis.

Tissue obtained from healthy lung explants was processed using a three-dimensional spheroid culture method, commonly used in the neural and cardiac fields. The spheroid culture process has been shown to be an effective method to take unsorted cell outgrowth from a biopsy and output progenitor cells [59], [60]. In other stem cell production methods which involve an extraction from a patient, cellular sorting through antigenic or chemical means is required to remove the non-progenitor cells before treatment. The spheroid method limits the need for manipulation, which decreases the risk for contamination and unexpected modifications of the cells. In cardiac treatment, the spheroid process has been used as a progenitor cell production method for the treatment of myocardial infarction using adult cardiac stem cells [42], [68]. The

use of sphere culture process has been applied in lungs mainly for cancer cell culture [79]. Also, three-dimensional spheres have been generated when culturing alveolar type II cells with known stromal support cells in a matrix substrate and dubbed alveolospheres [3]. In this thesis study, the spheroid culture process was applied successfully in the generation of adult lung progenitor cells. From an initial biopsy-sized tissue explant, LSCs were expanded to yield amounts viable for use in clinical treatments of chronic lung disease (Figure 3, Figure 4).

During the spheroid culture process, the cells spontaneously aggregate into three-dimensional spheres, which were analyzed using immunofluorescence to show the phenotypic localization of cells within the individual spheres. Within the sphere, the cellular composition closely matches the expression profile of adult epithelial lung cell markers, Pro-SP-C and CCSP. The cells making up the outer edge of the sphere show an increased presence of mesenchymal markers CD90 and CD105 (Figure 5). This architecture suggests that the cells are recapitulating the natural structure of the lung, with the epithelial progenitor cells being surrounded by supporting stromal and mesenchymal cells. This finding is similar to results found using the spheroid culturing method (Figure 5). By forming this structure, the support cells can recreate the signaling of the mesenchymal layer and lead to an increase in the stem cell-like characteristics of the internal cells.

The LSCs which result from the spheroid culture process also express adult lung progenitor markers Pro-SP-C and CCSP, mixed with mesenchymal markers CD90 and CD105, keeping the expression constant across the culture method and expansion. LSCs were expanded up to passage eight without a change in phenotype as confirmed with flow cytometry analysis.

Through cytometric analysis on dual-stained cells for both airway and alveolar progenitor markers Pro-SP-C and CCSP, a portion of the cellular population was identified within the LSCs which may represent bronchioalveolar stem cells as reported before (Figure 6) [1].

Being able to generate LSCs which express known lung progenitor cell markers at viable therapeutic numbers grants the opportunity to lead to effective stem cell treatments of diseases which damage the major anatomical regions of the lung. Before LSC treatment can reach the clinical stage, multiple *in vitro* and *in vivo* trials must be run to show safety and efficacy. Initial proof of concept assays were performed to further validate the use of LSCs.

Proof of therapeutic effect was shown through the use of a bleomycin-induced pulmonary fibrosis model in severe combined immunodeficient (SCID) mice. The use of SCID mice is required to avoid immune response to the injection of the human cells leading to unexpected rejections. Instilling bleomycin directly into the lungs through intratracheal injection leads to an increased inflammatory response and fibrous collagen production (Figure 8). Based on the striking difference in the results of the saline treatment control and sham group, the bleomycin was effective at generating the necessary pulmonary damage required for the model to be effective. At the macroscopic level, the LSC treatment post bleomycin injury is much more similar to the sham surgery group in comparison to the saline control, suggesting that the overall damage is decreased after LSC injection (Figure 8, top row). Histologically, this result is verified based on Ashcroft scoring, infiltrate measurement, and immunofluorescent assays. The Ashcroft score grades the overall fibrosis caused by bleomycin injury [69]. Scoring of the three groups show that the LSC treated group has a decreased

fibrotic score similar to the sham group after injury, suggesting a positive effect of the LSCs (Figure 8, bottom left). Translationally, decreased fibrosis can also lead to a decrease in progression of the fibrotic damage, based on the known cyclic inflammatory cycle [12]. Along with the Ashcroft scoring, a tissue infiltrate measure was taken based on the histology samples. Tissue infiltration measurements quantify the amount of abnormal deposition within a cellular structure [54]. In the case of pulmonary fibrosis, inflammatory responses leads to the deposition of fibrotic tissue and an influx of immune cells to the region, exacerbating the inflammatory/fibrotic cycle [80]. Less infiltration in the sham and treatment group compared to the saline treatment control indicates that the LSCs are reducing the effects of bleomycin on the lung and limiting the inflammatory reactions (Figure 8, bottom right). Other assays performed showed decreased apoptosis of cells in lungs treated with LSCs and the promotion of angiogenesis, most strikingly in the region near LSC engraftment (Figure 9). A notable finding in the LSC-treated lungs is that LSCs labeled with DiO are not well represented in the lung samples at the two week time point (Figure 9). This result is similar to what has been seen in previous work with cardiac spheroid cell treatments [44], [81]. Based on this result, it is more likely that the mode of action LSCs function through is a paracrine effect instead of engraftment and reconstruction of damaged tissue.

To compare LSC treatment to the current standard of stem cell therapies, MSCs, a syngeneic rat model was used. While both the AD-MSCs and LSCs proved effective at decreasing the fibrotic effects of bleomycin, the LSCs outperformed the AD-MSCs on all accounts, measuring lower on the Ashcroft score and the tissue infiltrate count (Figure 10).

While showing therapeutic effect of LSCs in an animal model of pulmonary fibrosis provides a proof of concept for potential future treatment, the actual mode of action of the benefits requires further elucidation before LSC can be moved into a more clinical setting. As stated above, the LSCs are attaching to the native lung tissue in a limited fashion so the primary mode of action must be a non-engraftment effect, such as paracrine signaling. While the full mechanism still requires further research to more thoroughly understand the signaling pathways and factors which lead to the therapeutic benefit, an initial study was performed to assess the therapeutic resemblance of the LSC secretome in comparison to the LSCs. Human lung epithelial cells were cultured *in vitro* and then assaulted with a bleomycin addition, leading to cellular damage. Treatment of the damaged cells with LSC-conditioned media led to a decrease in apoptosis in comparison to IMDM treated controls, which mimics the earlier *in vivo* result (Figure 12). When human umbilical vein endothelial cells were cultured on Matrigel with LSC-conditioned media versus control, greater tube length was measured (Figure 12). These *in vitro* results uphold the *in vivo* work described earlier and provide some initial data in regards to the potential mechanism of LSCs.

CHAPTER 3: CONCLUSION AND FUTURE WORK

The work presented in this thesis describes the use of a well-characterized culture method for increasing the overall stemness of cells acquired through tissue explantation and digestion in the human lung. With the growing use of stem cells in clinical therapeutic applications, a robust method for the generation of functional stem cells is required for the needs of patients. Stem cells provide the potential opportunity for more focused therapeutics for chronic pulmonary diseases, such as pulmonary fibrosis, which currently have no cure and treatments are limited to delaying the progression of the disease and increasing the overall quality of life. While the focus of this research has been on the use of mesenchymal stem cells which are easy to acquire and expand, the discovery of local niches of tissue specific stem cells has started to push future work towards adult stem cells. With the discovery of ATII and club cells as adult lung progenitor cells, the use of adult stem cells has become possible for chronic lung diseases. Through the use of the spheroid culture process, lung progenitor cells have been acquired in viable clinical numbers for treatment of pulmonary fibrosis. As an initial proof of concept, a rodent study was performed to verify that this cellular mixture is a viable therapy for pulmonary fibrosis. Although an initial study indicated that paracrine mechanisms may have a major responsibility for the beneficial effects of the LSC, further research is required to specify the important factors in the LSC secretome and understand the signaling interactions that occur in the fibrotic lung before LSC-derived proteins can be translated to further clinical progression.

REFERENCES

- [1] C. F. Bender Kim, E. L. Jackson, A. E. Woolfenden, S. Lawrence, I. Babar, S. Vogel, D. Crowley, R. T. Bronson, and T. Jacks, “Identification of bronchioalveolar stem cells in normal lung and lung cancer,” *Cell*, vol. 121, pp. 823–835, 2005.
- [2] T. J. Desai, D. G. Brownfield, and M. A. Krasnow, “Alveolar progenitor and stem cells in lung development, renewal and cancer,” *Nature*, vol. 507, no. 7491, pp. 190–194, Mar. 2014.
- [3] C. E. Barkauskas, M. J. Counce, C. R. Rackley, E. J. Bowie, D. R. Keene, B. R. Stripp, S. H. Randell, P. W. Noble, and B. L. Hogan, “Type 2 alveolar cells are stem cells in adult lung,” *J Clin Invest*, vol. 123, no. 7, pp. 3025–3036, 2013.
- [4] S. A. E. M. L. Nazir, “Chronic Obstructive Pulmonary Disease: An Update on Diagnosis and Management Issues in Older Adults. .”
- [5] S. R. Durrani, R. K. Viswanathan, and W. W. Busse, “What effect does asthma treatment have on airway remodeling? Current perspectives.,” *J. Allergy Clin. Immunol.*, vol. 128, no. 3, pp. 439–48; quiz 449–50, Sep. 2011.
- [6] S. Bozinovski, D. Anthony, and R. Vlahos, “Targeting pro-resolution pathways to combat chronic inflammation in COPD.,” *J. Thorac. Dis.*, vol. 6, no. 11, pp. 1548–56, Nov. 2014.
- [7] D. Siniscalco, N. Sullo, S. Maione, F. Rossi, and B. D’Agostino, “Stem cell therapy: the great promise in lung disease.,” *Ther. Adv. Respir. Dis.*, vol. 2, pp. 173–177, 2008.
- [8] A. M. Cantin, D. Hartl, M. W. Konstan, and J. F. Chmiel, “Inflammation in cystic fibrosis lung disease: Pathogenesis and therapy.,” *J. Cyst. Fibros.*, Mar. 2015.
- [9] D. H. MacIver and A. L. Clark, “The Vital Role of the Right Ventricle in the Pathogenesis of Acute Pulmonary Edema,” *Am. J. Cardiol.*, vol. 115, no. 7, pp. 992–1000, Apr. 2015.
- [10] G. Raghu, D. Weycker, J. Edelsberg, W. Z. Bradford, and G. Oster, “Incidence and prevalence of idiopathic pulmonary fibrosis.,” *Am. J. Respir. Crit. Care Med.*, vol. 174, no. 7, pp. 810–6, Oct. 2006.
- [11] M. Decramer, W. Janssens, and M. Miravittles, “Chronic obstructive pulmonary disease.,” *Lancet*, vol. 379, no. 9823, pp. 1341–51, Apr. 2012.

- [12] H. J. Kim, D. Perlman, and R. Tomic, “Natural history of idiopathic pulmonary fibrosis.,” *Respir. Med.*, Feb. 2015.
- [13] W. Li, Y. Zhao, Z. Sun, X. Yang, L. Zhao, and J. Shen, “Lung protective effects of budesonide nebulization during perioperative period of thoracolumbar fusion.,” *J. Thorac. Dis.*, vol. 6, no. 12, pp. 1800–7, Dec. 2014.
- [14] J. Fingleton, J. Travers, M. Williams, T. Charles, D. Bowles, R. Strik, P. Shirtcliffe, M. Weatherall, and R. Beasley, “Treatment responsiveness of phenotypes of symptomatic airways obstruction in adults.,” *J. Allergy Clin. Immunol.*, Mar. 2015.
- [15] R. A. Pleasants, H. Herrick, and W. Liao, “The prevalence, characteristics, and impact of chronic obstructive pulmonary disease in North Carolina.,” *N. C. Med. J.*, vol. 74, no. 5, pp. 376–83, Jan. .
- [16] L. Sonstein, C. Clark, S. Seidensticker, L. Zeng, and G. Sharma, “Improving adherence for management of acute exacerbation of chronic obstructive pulmonary disease.,” *Am. J. Med.*, vol. 127, no. 11, pp. 1097–104, Nov. 2014.
- [17] A. Tzouveleakis, F. Bonella, and P. Spagnolo, “Update on therapeutic management of idiopathic pulmonary fibrosis.,” *Ther. Clin. Risk Manag.*, vol. 11, pp. 359–370, Jan. 2015.
- [18] F. Hilberg, G. J. Roth, M. Krssak, S. Kautschitsch, W. Sommergruber, U. Tontsch-Grunt, P. Garin-Chesa, G. Bader, A. Zoepfel, J. Quant, A. Heckel, and W. J. Rettig, “BIBF 1120: triple angiokine inhibitor with sustained receptor blockade and good antitumor efficacy.,” *Cancer Res.*, vol. 68, no. 12, pp. 4774–82, Jun. 2008.
- [19] L. Richeldi, U. Costabel, M. Selman, D. S. Kim, D. M. Hansell, A. G. Nicholson, K. K. Brown, K. R. Flaherty, P. W. Noble, G. Raghu, M. Brun, A. Gupta, N. Juhel, M. Klüglich, and R. M. du Bois, “Efficacy of a tyrosine kinase inhibitor in idiopathic pulmonary fibrosis.,” *N. Engl. J. Med.*, vol. 365, no. 12, pp. 1079–87, Sep. 2011.
- [20] W. R. Coward, G. Saini, and G. Jenkins, “The pathogenesis of idiopathic pulmonary fibrosis.,” *Ther. Adv. Respir. Dis.*, vol. 4, no. 6, pp. 367–88, Dec. 2010.
- [21] L. Richeldi, V. Cottin, K. R. Flaherty, M. Kolb, Y. Inoue, G. Raghu, H. Taniguchi, D. M. Hansell, A. G. Nicholson, F. Le Maulf, S. Stowasser, and H. R. Collard, “Design of the INPULSIS™ trials: two phase 3 trials of nintedanib in patients with idiopathic pulmonary fibrosis.,” *Respir. Med.*, vol. 108, no. 7, pp. 1023–30, Jul. 2014.

- [22] J. T. Allen and M. A. Spiteri, "Growth factors in idiopathic pulmonary fibrosis: relative roles.," *Respir. Res.*, vol. 3, p. 13, Jan. 2002.
- [23] A. Di Sario, E. Bendia, G. Svegliati Baroni, F. Ridolfi, A. Casini, E. Ceni, S. Saccomanno, M. Marzioni, L. Trozzi, P. Sterpetti, S. Taffetani, and A. Benedetti, "Effect of pirfenidone on rat hepatic stellate cell proliferation and collagen production," *J. Hepatol.*, vol. 37, no. 5, pp. 584–591, Nov. 2002.
- [24] T. E. King, W. Z. Bradford, S. Castro-Bernardini, E. A. Fagan, I. Glaspole, M. K. Glassberg, E. Gorina, P. M. Hopkins, D. Kardatzke, L. Lancaster, D. J. Lederer, S. D. Nathan, C. A. Pereira, S. A. Sahn, R. Sussman, J. J. Swigris, and P. W. Noble, "A phase 3 trial of pirfenidone in patients with idiopathic pulmonary fibrosis.," *N. Engl. J. Med.*, vol. 370, no. 22, pp. 2083–92, May 2014.
- [25] X. Lin, M. Yu, K. Wu, H. Yuan, and H. Zhong, "Effects of pirfenidone on proliferation, migration, and collagen contraction of human Tenon's fibroblasts in vitro.," *Invest. Ophthalmol. Vis. Sci.*, vol. 50, no. 8, pp. 3763–70, Aug. 2009.
- [26] E. Loveman, V. R. Copley, J. L. Colquitt, D. A. Scott, A. J. Clegg, J. Jones, K. M. A. O'Reilly, S. Singh, C. Bausewein, and A. Wells, "The effectiveness and cost-effectiveness of treatments for idiopathic pulmonary fibrosis: systematic review, network meta-analysis and health economic evaluation.," *BMC Pharmacol. Toxicol.*, vol. 15, p. 63, Jan. 2014.
- [27] F. Hilberg, U. Tontsch-Grunt, F. Colbatzky, A. Heckel, R. Lotz, J. C. A. van Meel, and G. J. Roth, "158 BIBF1120 a novel, small molecule triple angiokinase inhibitor: profiling as a clinical candidate for cancer therapy," *Eur. J. Cancer Suppl.*, vol. 2, no. 8, p. 50, Sep. 2004.
- [28] M. Barczyk, M. Schmidt, and S. Mattoli, "Stem Cell-Based Therapy in Idiopathic Pulmonary Fibrosis.," *Stem Cell Rev.*, Apr. 2015.
- [29] K. Takahashi, K. Tanabe, M. Ohnuki, M. Narita, T. Ichisaka, K. Tomoda, and S. Yamanaka, "Induction of pluripotent stem cells from adult human fibroblasts by defined factors.," *Cell*, vol. 131, no. 5, pp. 861–72, Nov. 2007.
- [30] Q. Yan, Y. Quan, H. Sun, X. Peng, Z. Zou, J. L. Alcorn, R. a. Wetsel, and D. Wang, "A site-specific genetic modification for induction of pluripotency and subsequent isolation of derived lung alveolar epithelial type II cells," *Stem Cells*, vol. 32, pp. 402–413, 2014.

- [31] X. Liu, J. Chen, W. Liu, X. Li, Q. Chen, T. Liu, S. Gao, and M. Deng, "The fused in sarcoma protein forms cytoplasmic aggregates in motor neurons derived from integration-free induced pluripotent stem cells generated from a patient with familial amyotrophic lateral sclerosis carrying the FUS-P525L mutation.," *Neurogenetics*, Apr. 2015.
- [32] H. Zhang, C. Xue, R. Shah, K. Bermingham, C. C. Hinkle, W. Li, A. Rodrigues, J. Tabita-Martinez, J. S. Millar, M. Cuchel, E. Pashos, Y. Liu, R. Yan, W. Yang, S. J. Gosai, D. VanDorn, S. Chou, B. D. Gregory, E. Morrissey, M. Li, D. J. Rader, and M. P. Reilly, "Functional Analysis and Transcriptomic Profiling of iPSC-Derived Macrophages and Their Application in Modeling Mendelian Disease.," *Circ. Res.*, p. CIRCRESAHA.117.305860–, Apr. 2015.
- [33] F. Griscelli, O. Féraud, N. Oudrhiri, E. Gobbo, I. Casal, J.-C. Chomel, I. Bièche, P. Duvillard, P. Opolon, A. G. Turhan, and A. Bennaceur-Griscelli, "Malignant germ cell-like tumors, expressing Ki-1 antigen (CD30), are revealed during in vivo differentiation of partially reprogrammed human-induced pluripotent stem cells.," *Am. J. Pathol.*, vol. 180, no. 5, pp. 2084–96, May 2012.
- [34] D. Steinemann, G. Göhring, and B. Schlegelberger, "Genetic instability of modified stem cells - a first step towards malignant transformation?," *Am. J. Stem Cells*, vol. 2, no. 1, pp. 39–51, Jan. 2013.
- [35] M. Nakano-Okuno, B. R. Borah, and I. Nakano, "Ethics of iPSC-based clinical research for age-related macular degeneration: patient-centered risk-benefit analysis.," *Stem Cell Rev.*, vol. 10, no. 6, pp. 743–52, Dec. 2014.
- [36] D. Kim, C.-H. Kim, J.-I. Moon, Y.-G. Chung, M.-Y. Chang, B.-S. Han, S. Ko, E. Yang, K. Y. Cha, R. Lanza, and K.-S. Kim, "Generation of human induced pluripotent stem cells by direct delivery of reprogramming proteins.," *Cell Stem Cell*, vol. 4, no. 6, pp. 472–6, Jun. 2009.
- [37] D. Cyranoski, "Next-generation stem cells cleared for human trial," *Nature*, Sep. 2014.
- [38] T. Asahara, C. Kalka, and J. M. Isner, "Stem cell therapy and gene transfer for regeneration.," *Gene Ther.*, vol. 7, no. 6, pp. 451–7, Mar. 2000.
- [39] H. Ohgushi and A. I. Caplan, "Stem cell technology and bioceramics: from cell to gene engineering.," *J. Biomed. Mater. Res.*, vol. 48, no. 6, pp. 913–27, Jan. 1999.

- [40] P. Bianco, P. G. Robey, and P. J. Simmons, "Mesenchymal stem cells: revisiting history, concepts, and assays.," *Cell Stem Cell*, vol. 2, no. 4, pp. 313–9, Apr. 2008.
- [41] S. Wang, X. Qu, and R. C. Zhao, "Clinical applications of mesenchymal stem cells.," *J. Hematol. Oncol.*, vol. 5, no. 1, p. 19, Jan. 2012.
- [42] T.-S. Li, K. Cheng, S.-T. Lee, S. Matsushita, D. Davis, K. Malliaras, Y. Zhang, N. Matsushita, R. R. Smith, and E. Marbán, "Cardiospheres recapitulate a niche-like microenvironment rich in stemness and cell-matrix interactions, rationalizing their enhanced functional potency for myocardial repair.," *Stem Cells*, vol. 28, no. 11, pp. 2088–98, Nov. 2010.
- [43] R. R. Smith, L. Barile, H. C. Cho, M. K. Leppo, J. M. Hare, E. Messina, A. Giacomello, M. R. Abraham, and E. Marbán, "Regenerative potential of cardiosphere-derived cells expanded from percutaneous endomyocardial biopsy specimens," *Circulation*, vol. 115, pp. 896–908, 2007.
- [44] T. S. Li, K. Cheng, K. Malliaras, R. R. Smith, Y. Zhang, B. Sun, N. Matsushita, A. Blusztajn, J. Terrovitis, H. Kusuoka, L. Marbán, and E. Marbán, "Direct comparison of different stem cell types and subpopulations reveals superior paracrine potency and myocardial repair efficacy with cardiosphere-derived cells," *J. Am. Coll. Cardiol.*, vol. 59, no. 10, pp. 942–953, 2012.
- [45] S. J. Morrison and A. C. Spradling, "Stem cells and niches: mechanisms that promote stem cell maintenance throughout life.," *Cell*, vol. 132, no. 4, pp. 598–611, Feb. 2008.
- [46] A. Spradling, D. Drummond-Barbosa, and T. Kai, "Stem cells find their niche.," *Nature*, vol. 414, no. 6859, pp. 98–104, Nov. 2001.
- [47] G. Cotsarelis, T.-T. Sun, and R. M. Lavker, "Label-retaining cells reside in the bulge area of pilosebaceous unit: Implications for follicular stem cells, hair cycle, and skin carcinogenesis," *Cell*, vol. 61, no. 7, pp. 1329–1337, Jun. 1990.
- [48] L. Li and T. Xie, "Stem cell niche: structure and function.," *Annu. Rev. Cell Dev. Biol.*, vol. 21, pp. 605–31, Jan. 2005.
- [49] A. Giangreco, M. Qin, J. E. Pintar, and F. M. Watt, "Epidermal stem cells are retained in vivo throughout skin aging.," *Aging Cell*, vol. 7, no. 2, pp. 250–9, Mar. 2008.
- [50] A. Scopelliti, J. B. Cordero, F. Diao, K. Strathdee, B. H. White, O. J. Sansom, and M. Vidal, "Local control of intestinal stem cell homeostasis by enteroendocrine cells in the adult *Drosophila* midgut.," *Curr. Biol.*, vol. 24, no. 11, pp. 1199–211, Jun. 2014.

- [51] B. L. M. Hogan, C. E. Barkauskas, H. A. Chapman, J. A. Epstein, R. Jain, C. C. W. Hsia, L. Niklason, E. Calle, A. Le, S. H. Randell, J. Rock, M. Snitow, M. Krummel, B. R. Stripp, T. Vu, E. S. White, J. A. Whitsett, and E. E. Morrisey, "Repair and regeneration of the respiratory system: complexity, plasticity, and mechanisms of lung stem cell function.," *Cell Stem Cell*, vol. 15, no. 2, pp. 123–38, Aug. 2014.
- [52] J. D. Crapo, B. E. Barry, L. Y. Chang, and R. R. Mercer, "Alterations in lung structure caused by inhalation of oxidants.," *J. Toxicol. Environ. Health*, vol. 13, no. 2–3, pp. 301–21, Jan. 1984.
- [53] R. A. Wetsel, D. Wang, and D. G. Calame, "Therapeutic potential of lung epithelial progenitor cells derived from embryonic and induced pluripotent stem cells.," *Annu. Rev. Med.*, vol. 62, pp. 95–105, Jan. 2011.
- [54] P. R. Reynolds, R. E. Schmitt, S. D. Kasteler, A. Sturrock, K. Sanders, A. Bierhaus, P. P. Nawroth, R. Paine, and J. R. Hoidal, "Receptors for advanced glycation end-products targeting protect against hyperoxia-induced lung injury in mice.," *Am. J. Respir. Cell Mol. Biol.*, vol. 42, no. 5, pp. 545–51, May 2010.
- [55] E. L. Rawlins, T. Okubo, Y. Xue, D. M. Brass, R. L. Auten, H. Hasegawa, F. Wang, and B. L. M. Hogan, "The role of Scgb1a1+ Clara cells in the long-term maintenance and repair of lung airway, but not alveolar, epithelium.," *Cell Stem Cell*, vol. 4, no. 6, pp. 525–34, Jun. 2009.
- [56] J. G. Widdicombe and R. J. Pack, "The Clara cell.," *Eur. J. Respir. Dis.*, vol. 63, no. 3, pp. 202–20, May 1982.
- [57] S. D. Reynolds and A. M. Malkinson, "Clara cell: progenitor for the bronchiolar epithelium.," *Int. J. Biochem. Cell Biol.*, vol. 42, no. 1, pp. 1–4, Jan. 2010.
- [58] D. V LaBarbera, B. G. Reid, and B. H. Yoo, "The multicellular tumor spheroid model for high-throughput cancer drug discovery.," *Expert Opin. Drug Discov.*, vol. 7, no. 9, pp. 819–30, Sep. 2012.
- [59] E. Fennema, N. Rivron, J. Rouwkema, C. van Blitterswijk, and J. De Boer, "Spheroid culture as a tool for creating 3D complex tissues," *Trends Biotechnol.*, vol. 31, no. 2, pp. 108–115, 2013.
- [60] R. E. Durand, "Multicell spheroids as a model for cell kinetic studies.," *Cell Tissue Kinet.*, vol. 23, no. 3, pp. 141–59, May 1990.

- [61] L. P. Deleyrolle and B. A. Reynolds, "Isolation, expansion, and differentiation of adult Mammalian neural stem and progenitor cells using the neurosphere assay.," *Methods Mol. Biol.*, vol. 549, pp. 91–101, Jan. 2009.
- [62] S. M. Hecht, "Bleomycin: New Perspectives on the Mechanism of Action 1," *J. Nat. Prod.*, vol. 63, no. 1, pp. 158–168, Jan. 2000.
- [63] M. Gharaee-Kermani, Y. Nozaki, K. Hatano, and S. H. Phan, "Lung interleukin-4 gene expression in a murine model of bleomycin-induced pulmonary fibrosis.," *Cytokine*, vol. 15, no. 3, pp. 138–47, Aug. 2001.
- [64] T. Hoshino, M. Okamoto, Y. Sakazaki, S. Kato, H. A. Young, and H. Aizawa, "Role of proinflammatory cytokines IL-18 and IL-1beta in bleomycin-induced lung injury in humans and mice.," *Am. J. Respir. Cell Mol. Biol.*, vol. 41, no. 6, pp. 661–70, Dec. 2009.
- [65] E. De Langhe, F. Cailotto, V. De Vooght, C. Aznar-Lopez, J. A. Vanoirbeek, F. P. Luyten, and R. J. U. Lories, "Enhanced endogenous bone morphogenetic protein signaling protects against bleomycin induced pulmonary fibrosis.," *Respir. Res.*, vol. 16, no. 1, p. 38, Jan. 2015.
- [66] M. Ito, H. Hiramatsu, K. Kobayashi, K. Suzue, M. Kawahata, K. Hioki, Y. Ueyama, Y. Koyanagi, K. Sugamura, K. Tsuji, T. Heike, and T. Nakahata, "NOD/SCID/gamma(c)(null) mouse: an excellent recipient mouse model for engraftment of human cells.," *Blood*, vol. 100, no. 9, pp. 3175–82, Nov. 2002.
- [67] G. Su, Y. Zhao, J. Wei, J. Han, L. Chen, Z. Xiao, B. Chen, and J. Dai, "The effect of forced growth of cells into 3D spheres using low attachment surfaces on the acquisition of stemness properties," *Biomaterials*, vol. 34, no. 13, pp. 3215–3222, Apr. 2013.
- [68] R. R. Makkar, R. R. Smith, K. Cheng, K. Malliaras, L. E. J. Thomson, D. Berman, L. S. C. Czer, L. Marbán, A. Mendizabal, P. V Johnston, S. D. Russell, K. H. Schuleri, A. C. Lardo, G. Gerstenblith, and E. Marbán, "Intracoronary cardiosphere-derived cells for heart regeneration after myocardial infarction (CADUCEUS): a prospective, randomised phase 1 trial.," *Lancet*, vol. 379, no. 9819, pp. 895–904, Mar. 2012.
- [69] R. H. Hübner, W. Gitter, N. E. El Mokhtari, M. Mathiak, M. Both, H. Bolte, S. Freitag-Wolf, and B. Bewig, "Standardized quantification of pulmonary fibrosis in histological samples," *Biotechniques*, vol. 44, no. 4, pp. 507–517, 2008.

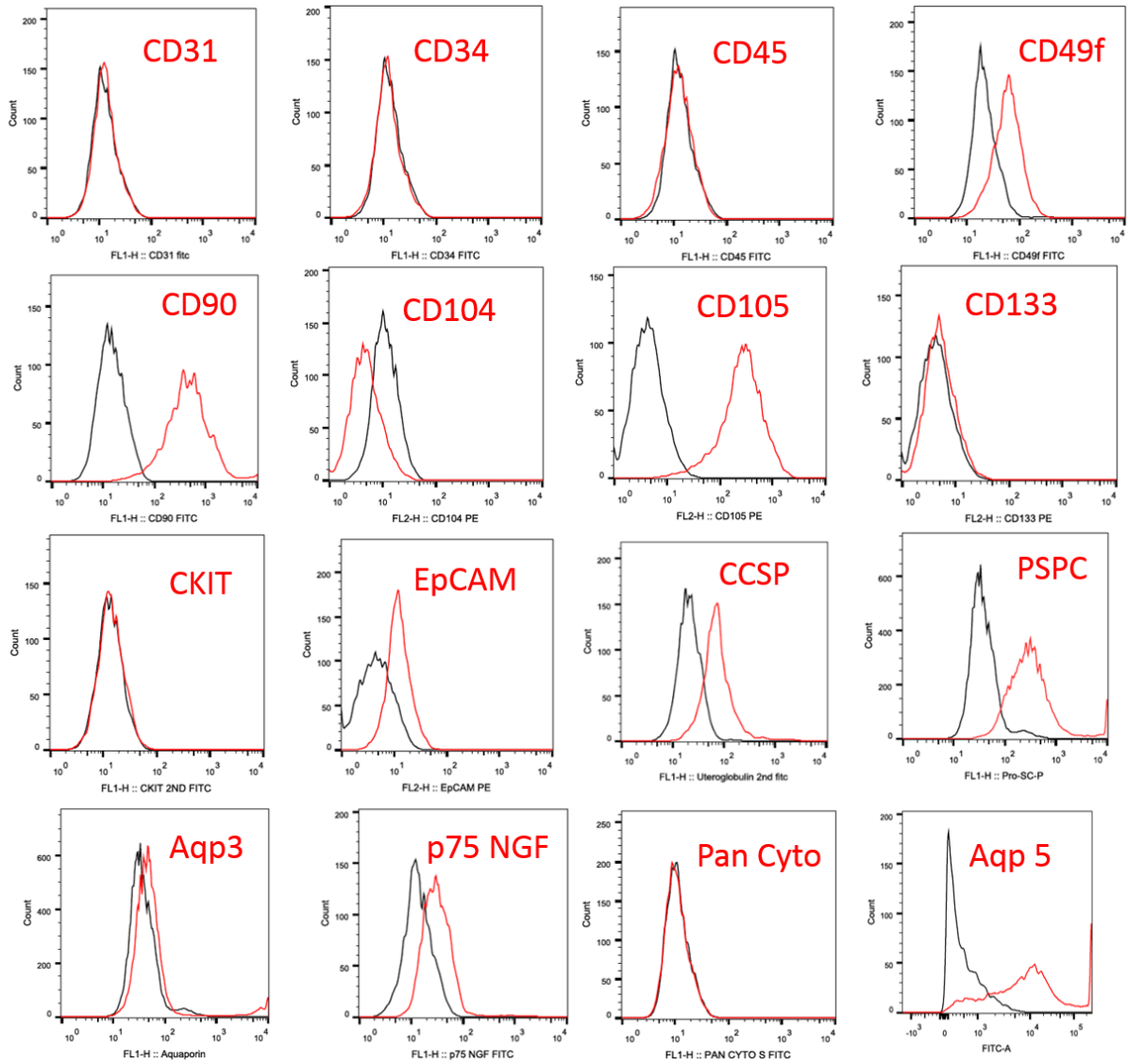
- [70] I. Arnaoutova and H. K. Kleinman, "In vitro angiogenesis: endothelial cell tube formation on gelled basement membrane extract.," *Nat. Protoc.*, vol. 5, no. 4, pp. 628–35, Apr. 2010.
- [71] I. Arnaoutova, J. George, H. K. Kleinman, and G. Benton, "The endothelial cell tube formation assay on basement membrane turns 20: state of the science and the art," *Angiogenesis*, vol. 12, no. 3, pp. 267–274, Apr. 2009.
- [72] Corning, "Primary Epithelial Ovarian Cancer Cells form Spheroids when Cultured on Corning® Ultra-Low Attachment Surfaces," *Corning - Cust. Appl. Note*, pp. 2–5.
- [73] E. Buzhor, O. Harari-Steinberg, D. Omer, S. Metsuyanin, J. Jacob-Hirsch, T. Noiman, Z. Dotan, R. S. Goldstein, and B. Dekel, "Kidney Spheroids Recapitulate Tubular Organoids Leading to Enhanced Tubulogenic Potency of Human Kidney-Derived Cells," Aug. 2011.
- [74] D. J. Weiss, R. Casaburi, R. Flannery, M. LeRoux-Williams, and D. P. Tashkin, "A placebo-controlled, randomized trial of mesenchymal stem cells in COPD.," *Chest*, vol. 143, no. 6, pp. 1590–8, Jun. 2013.
- [75] K. Le Blanc, F. Frassoni, L. Ball, F. Locatelli, H. Roelofs, I. Lewis, E. Lanino, B. Sundberg, M. E. Bernardo, M. Remberger, G. Dini, R. M. Egeler, A. Bacigalupo, W. Fibbe, and O. Ringdén, "Mesenchymal stem cells for treatment of steroid-resistant, severe, acute graft-versus-host disease: a phase II study.," *Lancet*, vol. 371, no. 9624, pp. 1579–86, May 2008.
- [76] I. Rajantie, M. Ilmonen, A. Alminaité, U. Ozerdem, K. Alitalo, and P. Salven, "Adult bone marrow-derived cells recruited during angiogenesis comprise precursors for periendothelial vascular mural cells.," *Blood*, vol. 104, no. 7, pp. 2084–6, Oct. 2004.
- [77] S. Fujiyama, K. Amano, K. Uehira, M. Yoshida, Y. Nishiwaki, Y. Nozawa, D. Jin, S. Takai, M. Miyazaki, K. Egashira, T. Imada, T. Iwasaka, and H. Matsubara, "Bone marrow monocyte lineage cells adhere on injured endothelium in a monocyte chemoattractant protein-1-dependent manner and accelerate reendothelialization as endothelial progenitor cells.," *Circ. Res.*, vol. 93, no. 10, pp. 980–9, Nov. 2003.
- [78] W. S. N. Shim, S. Jiang, P. Wong, J. Tan, Y. L. Chua, Y. S. Tan, Y. K. Sin, C. H. Lim, T. Chua, M. Teh, T. C. Liu, and E. Sim, "Ex vivo differentiation of human adult bone marrow stem cells into cardiomyocyte-like cells.," *Biochem. Biophys. Res. Commun.*, vol. 324, no. 2, pp. 481–8, Nov. 2004.

- [79] A. Amann, M. Zwierzina, G. Gamerith, M. Bitsche, J. M. Huber, G. F. Vogel, M. Blumer, S. Koeck, E. J. Pechriggl, J. M. Kelm, W. Hilbe, and H. Zwierzina, "Development of an innovative 3D cell culture system to study tumour--stroma interactions in non-small cell lung cancer cells.," *PLoS One*, vol. 9, no. 3, p. e92511, Jan. 2014.
- [80] K. Kuwano, N. Hagimoto, M. Kawasaki, T. Yatomi, N. Nakamura, S. Nagata, T. Suda, R. Kunitake, T. Maeyama, H. Miyazaki, and N. Hara, "Essential roles of the Fas-Fas ligand pathway in the development of pulmonary fibrosis.," *J. Clin. Invest.*, vol. 104, no. 1, pp. 13–9, Jul. 1999.
- [81] I. Chimenti, R. R. Smith, T. S. Li, G. Gerstenblith, E. Messina, A. Giacomello, and E. Marbán, "Relative roles of direct regeneration versus paracrine effects of human cardiosphere-derived cells transplanted into infarcted mice," *Circ. Res.*, vol. 106, no. 5, pp. 971–980, 2010.
- [82] LadyofHats. *Respiratory System Complete*. Open source image. Accessed from: http://en.wikipedia.org/wiki/Respiratory_system#/media/File:Respiratory_system_complete_en.svg. Accessed on May 2, 2015.

APPENDICES

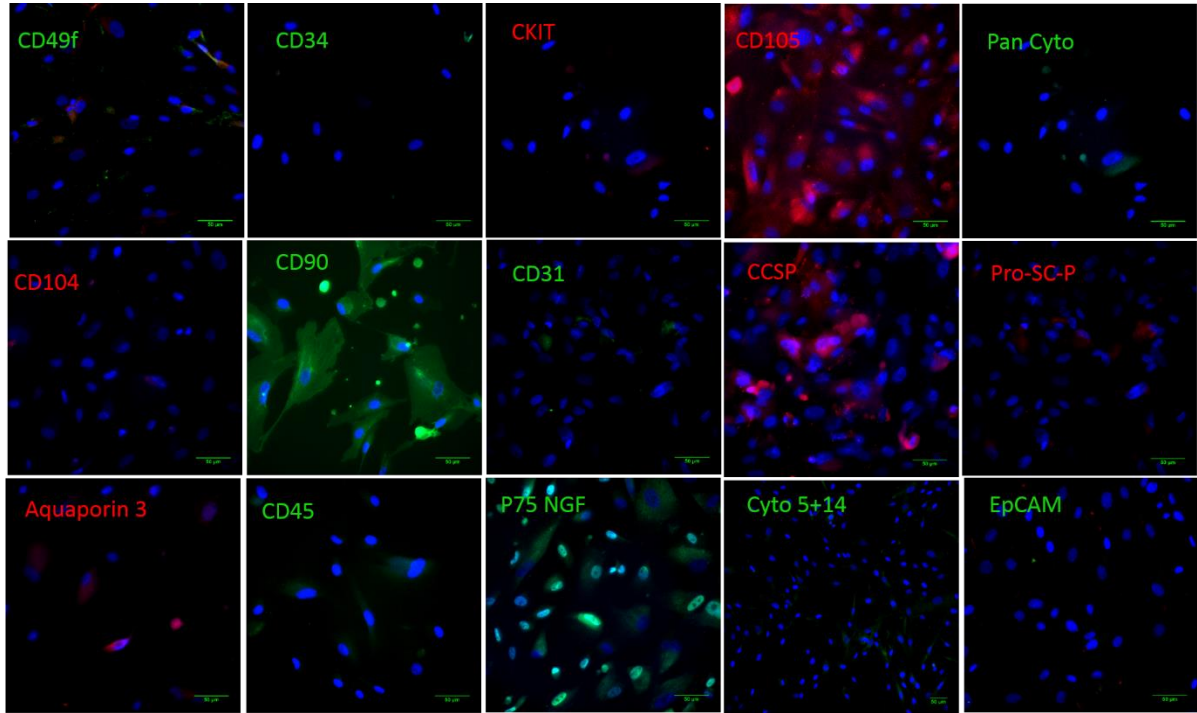
A. Supplementary Figures

A.1. Supplementary Figure 1



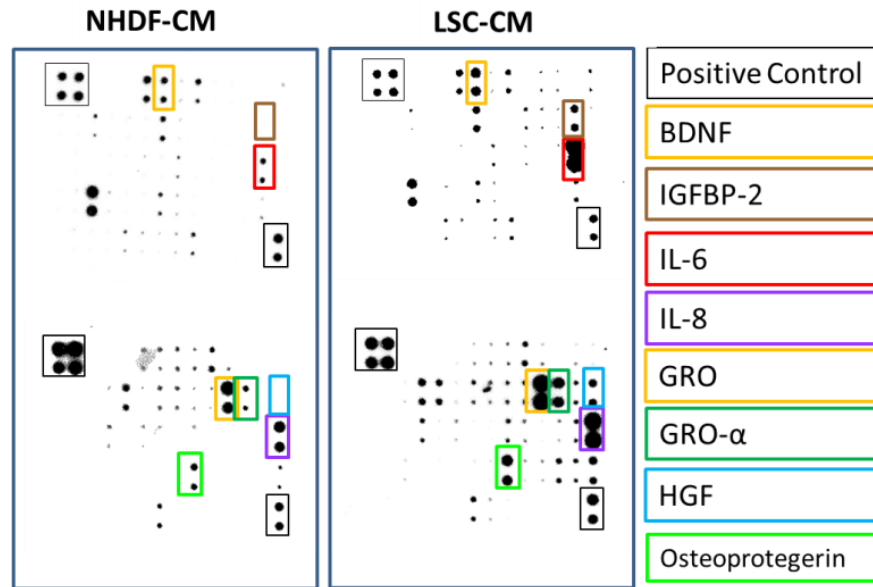
Supplementary Figure 1- Raw flow cytometry graphs for all analyzed markers vs. isotype control.

A.2. Supplementary Figure 2



Supplementary Figure 2- Immunofluorescence staining of cultured LSCs for multiple markers. Scale bar = 50 µm.

A.3. Supplementary Figure 3



Supplementary Figure 3- Cytokine array showing presence of proteins in LSC conditioned media versus Normal Human Dermal Fibroblasts (NHDF)

B. Supplementary Tables

B.1. Supplementary Table 1

	sex	age	race	cause of death	smoking
Lung Donor 1	Female	50	Hispanic	Anoxia 2 nd Cardiovascular	No
Lung Donor 2	Female	52	Black	Cerebrovascular Accident	No
Lung Donor 3	Male	18	Hispanic	Head Trauma 2nd Self-Inflicted Gunshot Wound	No

Supplementary Table 1- Lung donor information for the lung spheroid cells

B.2. Supplementary Table 2

Antibody	Vender	Product Number	Species	Isotype	Target
CD31	BD Biosciences	555445	Mouse	IgG _{1,κ}	Platelet endothelial cell adhesion molecule 1 (PECAM-1)
CD34	BD Biosciences	555821	Mouse	IgG _{1,κ}	Hematopoietic cell transmembrane glycoprotein antigen
CD45	BD Biosciences	555482	Mouse	IgG _{1,κ}	Leukocyte common antigen (LCA)
CD49f	BD Biosciences	555735	Rat	IgG _{2a,κ}	Integrin α6 transmembrane glycoprotein
CD90	BD Biosciences	555595	Mouse	IgG _{1,κ}	Thy-1 glycoposphatidylinositol- anchored membrane glycoprotein
CD90	Abcam	Ab92574	Rabbit	IgG	Thy-1 glycoposphatidylinositol- anchored membrane glycoprotein
CD90	Abcam	Ab23894	Mouse	IgG ₁	Thy-1 glycoposphatidylinositol- anchored membrane glycoprotein
CD90	Abcam	Ab225	Mouse	IgG ₁	Thy-1 glycoposphatidylinositol- anchored membrane glycoprotein
CD104	BD Biosciences	555720	Rat	IgG _{2b,κ}	Integrin β4 transmembrane glycoprotein
CD105	R&D Systems	Fab10971 p	Mouse	IgG ₁	Endoglin TGF-β receptor complex membrane glycoprotein
CD105	Abcam	Ab156756	Mouse	IgG _{2b}	Endoglin TGF-β receptor complex membrane glycoprotein
CD105	Abcam	Ab107595	Rabbit	IgG	Endoglin TGF-β receptor complex membrane glycoprotein
CD133	Miltenyi Biotec	120-000-425	Mouse	IgG _{1,κ}	Pentaspans transmembrane glycoprotein

CKIT	BD Biosciences	550412	Mouse	IgG _{1,κ}	Surface glycoprotein with tyrosine kinase activity present on hematopoietic progenitor cells
EpCAM	Abcam	Ab168828	Mouse	IgG ₁	Epithelial cell adhesion molecule transmembrane glycoprotein
P75 NGF	Abcam	Ab62122	Mouse	IgG _{2a}	Low affinity nerve growth factor neurotrophin receptor
CCSP (Uteroglobin)	Abcam	Ab40873	Rabbit	IgG	Club cell secretory protein
CCSP (Uteroglobin)	Abcam	Ab140663	Mouse	IgG ₁	Club cell secretory protein
Pro-SP-C	Abcam	Ab40879	Rabbit	IgG	Prosurfactant protein C
Pro-SP-C	Millipore	AB3786	Rabbit	Not listed	Prosurfactant protein C
Aquaporin 3	Abcam	Ab125219	Rabbit	IgG	Basolateral cell memberane
Cytokeratin 5+14	Abcam	Ab16570	Mouse	IgG _{2a}	Intermediate filaments of epithelial cells
Pan Cytokeratin	Abcam	Ab78478	Mouse	IgG ₁	Neoplastic epithelial cells
Aquaporin 5	Abcam	Ab85905	Rabbit	IgG	Pulmonary water channel membrane protein

Supplementary Table 2- List of antigenic markers used in analyses